



FACULTY OF ENGINEERING

POST-GRADUATE DIVISION

MASTER'S DEGREE IN HYDROCARBON PROCESSING ENGINEERING

DISSERTATION

---

Techno-Economic Comparative Analysis of Methanol Production via  
CO<sub>2</sub> Hydrogenation Using Different Kinetic Models

---

Author

---

Joaquim Paulo Samuel

Maputo, April 2025



EDUARDO MONDLANE UNIVERSITY

FACULTY OF ENGINEERING

POST-GRADUATE DIVISION

MASTER'S DEGREE IN HYDROCARBON PROCESSING ENGINEERING

DISSERTATION

---

Techno-Economic Comparative Analysis of Methanol Production via  
CO<sub>2</sub> Hydrogenation Using Different Kinetic Models

---

Author

---

Joaquim Paulo Samuel

Supervisor

---

Prof. Doutor João Chidamoio, Eng.

Maputo, April 2025

## TERM OF DELIVERY OF DISERTATION REPORT

I hereby declare that the finalist student Joaquim Paulo Samuel, delivered on \_\_\_\_/\_\_\_\_/20\_\_\_\_ as \_\_\_\_ copies of the Dissertation report with the reference: \_\_\_\_\_ with title Techno-economic Comparative Analysis of Methanol Production via CO<sub>2</sub> Hydrogenation Using Different Kinetic Models.

Maputo, \_\_\_\_ de \_\_\_\_\_ de 2024

The Head of Secretariat \_\_\_\_\_

## DECLARATION OF HONOR

I declare on my honor that the work presented below was carried out based on the knowledge acquired throughout the course and on the documents and references cited in it.

Maputo, April 2025

The author

---

(Joaquim Paulo Samuel)

## DEDICATION

I dedicate this work especially to my parents, Paulo Samuel Sigauque and Cristina David who have always supported and encouraged me in my studies. I also dedicate it to my brothers, friends and everyone who helped me achieve my goals.

## ACKNOWLEDGEMENT

First of all, I want to express my deepest gratitude to my parents, my father Paulo Samuel Sigauque and Cristina David, who have always encouraged and given me the strength to pursue my dreams. My heartfelt thanks also go to my wife, Luisa Francisco, and my children, Jaqueline Joaquim Sigauque and Ernesto Joaquim Sigauque, for being part of my life and motivating me every morning and night.

I would also like to extend my sincere thanks to the University members, starting with my supervisor, Prof. Dr. João Chidamoio, for supervising my dissertation, giving me invaluable advice, and encouraging me to be stronger and more consistent. A special thank you to Prof. Dr. Maria Eduardo, whom I consider my University mother. You gave me a second chance at life when I was in a critical situation, providing me with hope. To the secretarial staff, thank you all—Dr. Adileia, Eng. Inácio—for your support.

For the wonderful and challenging moments, my gratitude goes to my classmates. I want to start by saying, rest in peace Luisa Nyambir. You will forever remain in my memory—I still remember what you told me and taught me, and I thank you for everything. Thank you, Yannik Cossa, Salustiano Zavala, Joaquim Maunde, and Joecyline. I still remember when I wanted to give up, and you all hugged me, saying, “From now on, we are family; we will share the pain and support each other until the end.” We will forever be a family.

My final thanks go to Eduardo Mondlane University and Sasol Petroleum Temane for sponsoring the scholarship and internship program. The internship has opened doors for my professional career. Thank you very much!

## ABSTRACT

Methanol synthesis from carbon dioxide hydrogenation is finding applications across various industries. Many studies on methanol synthesis have been developed to enhance environmental suitability, with a focus on carbon dioxide reduction. However, studies in this area often rely on kinetic models based on catalyst data or experimental results. In the case of techno-economic studies, the scope typically does not include an investigation of kinetic models. Moreover, studies comparing techno-economic kinetic models are limited.

The main objective of this study was to conduct a techno-economic analysis of methanol production from CO<sub>2</sub> hydrogenation using different kinetic models. The methanol synthesis design was conducted in Aspen HYSYS V11, employing the equation of state (EoS) *Peng-Robinson*, *VBF*, *Ref-Graaf*, *Graaf*, and *Nestler* kinetic modes in a plug flow reactor. Heat integration and economic analysis were also performed using Aspen Energy Analyzer and Aspen Economic Evaluation.

The different performances in CO<sub>2</sub> conversion are related to thermodynamic parameters. Notably, the *Nestler* km showed the highest overall carbon conversion (76.71%), high methanol selectivity (55.81%), and 609.09 MW of recoverable heat, compared to the *Ref-Graaf* model. Both the *Nestler* and *Ref-Graaf* models were found to be techno-economically viable, excluding hydrogen costs, with LCM<sub>MeOH</sub> values of 308.34 M\$/yr for Nestler and 449.54 M\$/yr for Ref-Graaf. For the Nestler model, the cost of the hydrogen stream contributed 24.30% to the total OPEX, whereas, for Ref-Graaf, hydrogen cost accounted for 45.4% of the total OPEX.

In comparing the annual OPEX and LCM<sub>MeOH</sub> of the developed methanol plant using different kinetic models with and without the hydrogen stream, it was observed that the hydrogen stream significantly impacts both LCM<sub>MeOH</sub> and OPEX. *Ref-Graaf* and *Nestler*, as the most recent kinetic models, show potential for future sustainable methanol production due to their high methanol yield, selectivity, and economic viability.

Key-words: Techno-economic, comparative analysis, methanol, kinetic models

## RESUMO

A síntese de metanol a partir da hidrogenação do dióxido de carbono está encontrando aplicações em diversas indústrias. Muitos estudos sobre a síntese de metanol têm sido desenvolvidos com o objetivo de melhorar a adequação ambiental, focando na redução do dióxido de carbono. No entanto, estudos nesta área frequentemente dependem de modelos cinéticos baseados em dados de catalisadores ou resultados experimentais. No caso de estudos técnico-econômicos, o escopo geralmente não inclui uma investigação dos modelos cinéticos. Além disso, são limitados os estudos que comparam a análise técnico-econômicos dos modelos cinéticos.

O principal objetivo deste estudo foi realizar uma análise técnico-econômica da produção de metanol a partir da hidrogenação de CO<sub>2</sub> utilizando diferentes modelos cinéticos. O projeto de síntese de metanol foi conduzido no Aspen HYSYS V11, empregando a equação do estado de Peng-Robinson, e os modos cinéticos VBF, Ref-Graaf, Graaf e Nestler em um reator de fluxo tubular. A integração térmica e a análise econômica também foram realizadas utilizando o Aspen Energy Analyzer e o Aspen Economic Evaluation.

Os diferentes desempenhos na conversão de CO<sub>2</sub> estão relacionados a parâmetros termodinâmicos. Notavelmente, o modelo cinético de Nestler apresentou a maior conversão de carbono total (76,71%), alta seletividade para metanol (55,81%) e 609,09 MW de calor recuperável, em comparação com o modelo Ref-Graaf. Tanto os modelos Nestler quanto Ref-Graaf mostraram-se viáveis do ponto de vista técnico-econômico, excluindo os custos de hidrogênio, com valores de LCM<sub>OH</sub> de 308,34 M\$/ano para Nestler e 449,54 M\$/ano para Ref-Graaf. Para o modelo de Nestler, o custo da corrente de hidrogênio contribuiu com 24,30% do OPEX total, enquanto, para Ref-Graaf, o custo do hidrogênio representou 45,4% do OPEX total.

Ao comparar o OPEX anual e o LCM<sub>OH</sub> da planta de metanol desenvolvida usando diferentes modelos cinéticos, com e sem a corrente de hidrogênio, observou-se que a corrente de hidrogênio impacta significativamente tanto o LCM<sub>OH</sub> quanto o OPEX. Os modelos Ref-Graaf e Nestler, sendo os modelos cinéticos mais recentes, demonstram potencial para uma produção sustentável de metanol no futuro, devido ao seu alto rendimento de metanol, seletividade e viabilidade econômica.

**Palavras-chave:** Técnico-econômico, análise comparativa, metanol, modelos cinéticos.



## Contents

TERM OF DELIVERY OF DISERTATION REPORT .....	I
DECLARATION OF HONOR .....	II
DEDICATION .....	III
ACKNOWLEDGEMENT .....	IV
ABSTRACT.....	V
FIGURE CONTENTS .....	IX
TABLE CONTENTS.....	X
ACRONYM AND ABBREVIATION.....	XI
CHAPTER 1: INTRODUCTION .....	1
1.1. Background .....	1
1.2. Researcher Problem .....	2
1.3. Objectives .....	3
1.3.1. General objective .....	3
1.3.2. Specifics objectives:.....	3
1.4. Justification .....	3
CHAPTER 2 – LITERATURES REVIEWS .....	5
2.1. Methanol Production process.....	5
2.1.1. Methanol synthesis from natural gas.....	5
2.1.2. Methanol Synthesis from Coal and Bio-mass gasification .....	7
2.1.3. Methanol from catalytic hydrogenation of CO <sub>2</sub> .....	8
2.2. Methanol Kinetics Model.....	9
2.3. Commercial Technology for methanol Synthesis .....	12
2.3.1. High to low Pressure methanol synthesis.....	12
CHAPTAR 3 – METHODOLOGIES .....	14

3.1. Overview.....	14
3.1.1. Kinetic models schemes.....	15
3.2. Simulation process .....	22
3.2.1. Crude methanol Purification .....	24
3.2.2. Heat integration.....	24
3.2.3. Cost analyses.....	26
CHAPTER 4 – RESULTS AND DISCUSSION .....	28
4.1. Sensitivity Analysis study of kinetic models .....	28
4.1.1. Kinetic Model Validation.....	28
4.1.2. Overalls Carbon-conversion and per-pass conversion.....	33
4.2. Crude methanol Purification .....	35
4.2.1. Distillation performance .....	36
4.3. Energy and Economic Analysis .....	38
4.3.2. Economic Analysis .....	43
CHAPATER 5 – CONCLUSION, RECOMMENDATION AND LIMITATION .....	46
5.1. Conclusion .....	46
5.2. Recommendation .....	47
5.3. Limitation.....	47
BIBLIOGRAPHY .....	48

## FIGURE CONTENTS

Figure 1: Methanol Production based on Cu-ZnO-Al <sub>2</sub> O <sub>3</sub> catalyst (Li et al., 2022).....	9
Figure 2: Temperature profile of the commercial methanol technologies: (A) direct quenching (ICI), (B) indirect cooling ( Haldor Topsoe), and (C) quasi-isothermal BWR (Lurgi) (Bisotti et al., 2022). .....	13
Figure 3: Lurgi simulation Reactor flowsheet .....	22
Figure 4: Process flow diagrams of proposed kinetic models for methanol Production from CO <sub>2</sub> hydrogenation. ....	25
Figure 5: Simulation profile of non-adiabatic reactor of different kinetics model .....	28
Figure 6: Simulation of CO <sub>2</sub> -conversion profile at various kinetic models.....	29
Figure 7: Simulation CH <sub>3</sub> OH yield profile of various kinetic models.....	30
Figure 8: Simulation o H <sub>2</sub> - conversion profile of different kinetic models .....	30
Figure 9: Simulation of CO <sub>2</sub> to CO-conversion profile of each kinetic models.....	31
Figure 10: Simulation of H <sub>2</sub> O conversion profile of each kinetic models. ....	31
Figure 11: Temperature Profile of methanol synthesis of various kinetic models .....	32
Figure 12: Overalls carbon conversion of each kinetic models.....	34
Figure 13: Methanol and carbon monoxide selectivity of each kinetic models. ....	34
Figure 14: Column composition of (A)-VBF, (B)-Ref-Graaf, (C)-Graaf and (D)-Nestler KMs. ....	37
Figure 15: Column temperature profiles.....	38
Figure 16: The Heating and cooling Utilities energy and cost (E and F). ....	40
Figure 17: Total steam utilities (HEN) integrated (G) and the integrated utilities cost saved (H) .....	41
Figure 18: Energy performance of steam cooling VBF (I), Ref-Graaf (J), Graaf (K) and Nestler (L). ....	42
Figure 19: levelized cost of MeOH including cost of hydrogen in M\$ per tones of methanol. ..	43
Figure 20: levelized cost of MeOH without hydrogen cost in M\$ per tones of methanol. ....	43
Figure 21: Comparison of annual operational expense of the devoloped methanol plant using kinetic models tudy, total OPEX. ....	44
Figure 22: Comparison annual OPEX of the developed methanol plant using kinetic models without hydrogen cost.....	44

## TABLE CONTENTS

<b>Table 1:</b> The commonly kinetic model and recently proposed model .....	11
<b>Table 2:</b> The original kinetic and thermodynamic parameters for the considered kinetics, .....	16
Table 3: Reformulated reaction rate (Compliant with the Aspen HYSYS PFR reactor) .....	20
<b>Table 4:</b> Kinetic parameters of the reformulate model (activation energy in (J/mol)) .....	21
<b>Table 5:</b> Parameter of Adsorption constant-Adsorption energy in (J/mol).....	21
<b>Table 6:</b> Parameter proprieties of reactors, catalytic dimension and feed syngas composition...	23
<b>Table 7:</b> Estimation prices (US\$/MMScf) of natural gas of potential African countries .....	27
<b>Table 8:</b> Composition of reactor inlet and reactor product outlets( kmols/h).....	33
Table 11: crude methanol purification (Vent, recycle ratio, methanol and water) .....	35
<b>Table 12:</b> performance of column distillation, include Reflux ratio, feed and output composition .....	36
Table 13: Energy and Utility Consumption Comparison across Methanol Synthesis Models.....	39

## ACRONYM AND ABBREVIATION

$a$	descont rate
ART	Authothermal reforming
AVP	Advanced for Production
B	Adsorption constant
BASF	Badische Anilin und Soda Fabrik
BWR	Boiling Water Reactor
CAPEX	Captal Expenditures
CCS	Carbon Capture Storage
$C_k$	purchase cost
CO	Carbon monoxide
CO <sub>2</sub>	Carbon dioxide
COG	Coke oven gas
DC	Destilation Column
DCM	dimethyl carbonate
DEN	Denominator
E	Heater
$E_a$	Activation Energy
EoS	Equation of sate
fc	capacity factor
fe	surrounding factor
$F_i$	Consumption of Utilities
HE	Heat exchanger
HTS	High temperature synthesis
HX	Heater Exchanger
ICI	Imperial Chemical Industries
K(ads)	Adsorption constant
$K_{i,j}$	kinetic constants
KMs	Kinetic Models
LCMeOH	Levelized cost of Methanol
LHHW	Langmuir-Hinshelwood-Hougen-Wastson
LLT	Levelized life Time
LTS	Low Temperature Synthesis
M	module
M\$	Millions of dollar
MeOH	Methanol
MMBtu	million Brish therm Unit
mMeOH	mass of methanol
MMscf	meter stander cubic fit
Mt/yr	Million ton per year
MTBE	Methyl tertiary butyl ether
MTPD	Million ton per day

MW	mega watt
n	life time
NG	Natural gas
NT	Numerator
OPEX	Operation Expenditures
OPEX <sub>fixed</sub>	Operation Expenditures cost fixed
OPEX <sub>var</sub>	Operation Expenditures cost variation
Or-Graaf	Original Graaf
P	Pressure (bar)
PFR	Plug Flow Reactor
PO	Partial oxidation
PR	Peng-Rombson
PSA	Pressure Swing Adsorption
Pt	Production time
R	Rate equation
Ref-Graaf	Refitted Graaf
S	Stoichmetric
SMR	Steam methane reforming
SR	Steam reforming
STY	Selectivity
T	temperature (K)
V	Vessel
VBF	Vanden Bussche and Fromen
RWGS	Reverse Water gas shift
$\Delta T_{min}$ ,	Minima variation of temperature

## CHAPTER 1: INTRODUCTION

### 1.1. Background

The ongoing expansion and swift urbanization of the global population and economy have led to a substantial rise in energy requirements, prompting a shift from fossil-based fuels to cleaner renewable alternatives. As a result, achieving global decarbonization in key sectors such as transportation, industry, and electricity generation is imperative to address anthropogenic climate change. Within this framework, there is an increasing interest among scholars and industries in exploring versatile production routes such as hydrogen and methanol (Osman et al., 2022).

Methanol stands as a widely utilized and globally distributed substance, finding application across various industries. Its significance is underscored by the ongoing depletion of fossil fuel reserves, positioning it as an optimal alternative fuel in light of the rapid decline in oil and gas resources. In the realm of the chemical industry, methanol serves diverse commercial purposes, including the synthesis of formaldehyde, aromatics, ethylene, methyl tertiary butyl ether (MTBE), acetic acid, and other chemicals. Moreover, the demand for methanol is on the rise in fuel-related applications, encompassing the production of dimethyl carbonate (DMC), biodiesel manufacturing, direct blending into gasoline, and its potential as a conventional energy storage solution for fuel cell applications. Notably, methanol's appeal extends from its versatility to its cleaner emissions compared to conventional fossil fuel resources (Luyben, 2010; Zangeneh, Sahebdelfar, & Ravanchi, 2011).

In the contemporary manufacturing of methanol, the predominant technology relies on natural gas as the primary feedstock, although certain processes may utilize oil. This production involves a four-step procedure: syngas generation, compression, methanol synthesis, and distillation. Scientific advancements are increasingly focused on syngas generation and methanol synthesis. In a conventional methanol plant, approximately 55 % of the financial investment for process units is allocated to syngas generation. Various syngas production methods are available, dependent on the natural gas characteristics and economic constraints of the plant. These methods include steam reforming, autothermal reforming, and combined reforming (Bermúdez et al., 2013).

At present, the primary method for methanol production involves a commercial catalytic process utilizing carbon monoxide, carbon dioxide, and hydrogen. This process, pioneered by Imperial

Chemical Industries (ICI) in 1966, centers around the CO hydrogenation reaction occurring over a Cu/ZnO/Al<sub>2</sub>O<sub>3</sub> catalyst. The reaction takes place at relatively high temperatures and pressures, specifically in the range of 523–553 K and 60–80 bar, respectively. This established technique has become a cornerstone in the methanol manufacturing landscape (Kim et al., 2017).

The synthesis of methanol from synthesis gas (syngas) involves an exothermic reaction. The ICI process, known for its notably high reaction temperature, faces a thermodynamic constraint in achieving one-pass conversion, typically ranging from 15% to 25%. As a result, the process mandates the recycling of unreacted syngas and entails a significant cooling duty cycle. This operational necessity contributes to increased methanol production costs in specific setups. In response to this challenge, the research community has actively pursued the exploration of catalytic processes for low-temperature methanol synthesis. These investigations aim to overcome the difficulties associated with elevated reaction temperatures, ultimately improving the economic feasibility of methanol production processes (Kim et al., 2017).

## 1.2. Researcher Problem

Due studies that compare km's are based on catalyst studies or at least with access to experimental results, in the case of techno-economic studies, the scope does not include the investigation of the km's, and other hands, the studies that compare techno-economic km's are limited (Nyári et al., 2022).

This is due to the fact that kinetic modeling was in high request in techno-economic assessment studies as soon as interest in CO<sub>2</sub> utilization and power-to-methanol processes started growing (J. Portha et al., 2021; Bisotti et al., 2022). Revisiting the ancestors: Graaf and VBF models were modified or refitted over the years, but some of the pseudo-kinetic models of each are more suitable for methanol production. Basing on studies developed by Nyári et al., (2022) where the Kiss, Slotboom and VBF was studied and Bisotti et al., (2022), where original Graaf, ref-Graaf and VBF also was studied, and many of them are suitable for methanol synthesis, compared to the older KMs (Graaf and VBF).

However, the km's have high economically impacts - methanol synthesis from syngas and the process of methanol synthesis are governed by highly exothermal reaction; therefore, it is notably the process is high reaction temperature, faces a thermodynamic constraint in achieving one-pass conversion, typically ranging from 15 – 25 %, that same limitation of km proposed by



(Vanden Bussche & Froment, 1996). As a result, the process mandates the recycling of unreacted syngas and entails a significant cooling duty cycle (Kim et al., 2017). However, lowering the temperature of the process is not kinetically favorable, as it hampers the reaction rate. Therefore, a balance must be found between operating at elevated temperatures to enhance the reaction rate and lower temperatures to increase conversion. This challenge is addressed by employing reactors with recycling mechanisms to achieve complete 100 % conversion (Balopi, Agachi, & Danha, 2019; Huš, Dasireddy, Strah Štefančič, & Likozar, 2017). The reason why the objective of this study is to conduct a techno-economic comparative analysis of methanol production from CO<sub>2</sub> hydrogenation using different kinetic models.

### 1.3. Objectives

#### 1.3.1. General objective

The primary objective of this dissertation is to conduct the techno-economic comparative analysis of methanol production via CO<sub>2</sub> hydrogenation using different kinetic models.

#### 1.3.2. Specifics objectives:

The specific objectives of this dissertation are outlined as follows:

- Select kinetic models and validate them through initial simulation runs;
- Analyze the methanol yield, conversion, and selectivity for each kinetic model;
- Perform heat network integration to minimize the energy demand;
- Identify the economically viable kinetic model for methanol production.

### 1.4. Justification

In recent years, there has been a notable increase in anthropogenic emissions of CO<sub>2</sub>, a consequence of ongoing social and economic development. This surge has led to higher concentrations of greenhouse gases in the atmosphere, contributing to the global rise in temperatures. This issue persists as a worldwide concern. Consequently, various innovative strategies are being advocated to address CO<sub>2</sub> emissions, with a focus on capturing and injecting CO<sub>2</sub> underground as a mitigation measure (Nguyen & Zondervan, 2019).

A third alternative emerges in the synthesis of chemicals from fossil carbon using existing organic chemistry. In this approach, the CO<sub>2</sub> generated at the end of the product's life cycle is captured and

returned to the lithosphere, essentially reversing the carbon journey from fossil sources (Gabrielli et al., 2020). This process, known as Carbon Capture and Storage (CCS), involves safely storing CO<sub>2</sub> in suitable underground geological structures. Methanol stands out as a promising candidate in this context as an Advanced Vector for Production (AVP). Its role is significant due to its versatility as an intermediate in the chemical industry and its potential for storing a substantial amount of carbon. Moreover, the methanol synthesis process from syngas has reached a commercial stage, further highlighting its viability in the pursuit of sustainable carbon management (Portha et al., 2021; Gabrielli et al., 2020).

A compelling alternative to the conventional approach of CO<sub>2</sub> sequestration involves utilizing captured carbon as a reagent for the production of valuable chemicals. This can be achieved through various methods, including biological, chemical, or electrochemical processes. Currently, there is a growing interest in exploring the conversion of CO<sub>2</sub>, rather than mere sequestration, as a potential solution to mitigate CO<sub>2</sub> emissions into the atmosphere. The concept involves the production of value-added chemicals, such as ethanol, from CO<sub>2</sub>, providing a promising alternative to traditional petrochemical methods. This approach offers a dual benefit by not only repurposing CO<sub>2</sub> but also conserving fossil resources and mitigating emissions associated with their use (Olajire, 2013).

Therefore, Methanol is considered an excellent liquid H<sub>2</sub> source with low toxicity and low chain-alcohols. Compared to other fuels, methanol presents several advantages for hydrogen production. In fact, the absence of a strong C - C bond facilitates the reforming at low temperatures (200–300 °C), a range of temperatures that is very low when compared to other common fuels (800–1000 °C for methane and 400 °C for ethanol) For this reason, many research groups are developing various technologies that utilize methanol in the production of hydrogen (Dalena et al., 2018a). However, find the suitable kinetics models to methanol processing it can enhance environmental interest to sequester CO<sub>2</sub> to methanol synthesis.

## CHAPTER 2 – LITERATURES REVIEWS

### 2.1. Methanol Production process

Regarding Balopi et al., 2019, methanol production process starts with gasification of any solid carbon bearing matter i.e. coal, biomass or reforming of natural gas, to produce syngas (CO, CO<sub>2</sub> and H<sub>2</sub>) which is later used in the process to produce methanol via catalytic synthesis over Cu-based catalyst. Downstream of methanol synthesis is methanol purification stage where methanol is purified according to specifications from customers and other needs from the chemical industry. Therefore, in this chapter will be discussed in details the technology used to produce methanol from different carbon dioxide feedstock.

#### 2.1.1. Methanol synthesis from natural gas

Currently, the production of methanol heavily depends on a well-established technology that is mainly focused on natural gas, constituting 90% of the process. A small percentage of the global capacity comes from petroleum fractions and process off-gases. When natural gas serves as the feedstock, the essential procedure involves the following key steps: desulphurization of natural gas; synthesis gas generation; synthesis gas compression; methanol synthesis and methanol distillation (Ramon L. Espino & Pletzke, 1975; Dalena et al., 2018b).

Regarding Dalena et al., 2018b, empathize that, the mixture of syngas (H<sub>2</sub>, CO, and CO<sub>2</sub>) is mainly produced by steam reforming (SR) and autothermal reforming (ATR) of natural gas respectively. However, it is also obtained by partial oxidation (PO) of methane or different carbon-based materials such as coal, heavy oils, or biogas. On other hand, for methanol synthesis depends specifically of stoichiometric ratio of mixtures of the syngas (H<sub>2</sub> – CO<sub>2</sub>) / (CO + CO<sub>2</sub>), represented to as the module M. the module of 2 defines a stoichiometric gas for formation of methanol (Aasberg-Petersen et al., 2007). According Balopi et al., 2019; Palma, Meloni, Ruocco, Martino, & Ricca, 2018, stoichiometric number slightly larger than 2 appears to be optimal for most of catalysts used in industrial production of methanol. As reported by Dalena et al., 2018b, the stoichiometric value M takes into account the presence of CO<sub>2</sub> converted that consumes hydrogen via the reverse WGS reaction, represented in (Eq.1).



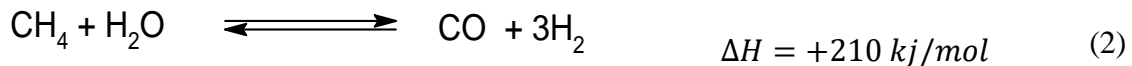
The different technologies for methanol production, from natural gas was discussed for many different authors. According to Aasberg-Petersen et al., 2007, several reforming technologies are available for production syngas: one-step reforming with fired tubular reforming; two-step reforming; and Autothermal reforming (ATR)

A majority of the methanol plants operating today are based on steam reforming of natural gas. This technology is attractive at capacities greater than 2500 – 30000 MTPD (Ramon L. Espino & Pletzke, 1975).

The Aasberg-Petersen et al., 2007, discussed the processes of one and two step reforming, and Autothermal reforming:

The first step of the SMR process involves methane reacting with steam at 750-800°C (1380-1470°F) to produce a synthesis gas (syngas), see (Eq.2) a mixture primarily made up of hydrogen (H<sub>2</sub>) and carbon monoxide (CO).

In the second step, known as a water gas shift (WGS) reaction, the carbon monoxide produced in the first reaction is reacted with steam over a catalyst to form hydrogen and carbon dioxide (CO<sub>2</sub>), see (Eq.3). This process occurs in two stages, consisting of a high temperature shift (HTS) at 350°C (662°F) and a low temperature shift (LTS) at 190-210°C (374-410°F) (NYSERDA, 2004). At section will be discussion the (HTS and LTS).



The equations presented indicate a surplus of hydrogen—more than what's necessary to convert carbon oxides into methanol. To address this, one potential solution involves introducing CO<sub>2</sub> to align with the excess hydrogen. This adjustment clearly diminishes the feed and fuel needs per ton of methanol. The inclusion of CO<sub>2</sub> into the reformer, alongside feed and steam, serves to elevate the CO to CO<sub>2</sub> ratio in the syngas. Consequently, this enhancement boosts carbon efficiency within the synthesis process (Ramon L. Espino & Pletzke, 1975).

According to Aasberg-Petersen et al., 2007, approximately 40 % of the hydrogen generated in the one-step reforming process is considered excessive. This surplus hydrogen traverses the synthesis section without undergoing reaction and requires purging. However, it is also utilized as reforming fuel in autothermal reforming.

The synthesis gas generated through autothermal reforming exhibits a heightened reactivity owing to its rich carbon monoxide content. With a module ranging from 1.7 to 1.8, the gas is deficient in hydrogen and needs adjustment to a value of approximately 2 for suitability in methanol production. This adjustment can be achieved by either removing carbon dioxide from the synthesis gas or by extracting hydrogen from the synthesis loop purge gas and reintroducing it into the synthesis gas. When CO<sub>2</sub> removal is employed, it yields a synthesis gas with an exceptionally high CO/CO<sub>2</sub> ratio, resembling the composition found in methanol plants relying on coal gasification. Alternatively, adjusting the module through hydrogen recovery can be accomplished using either a membrane or a PSA unit, both of which are well-established in the industry. The resulting synthesis gas from this type of module adjustment is less aggressive and may be preferable for the production of high-purity methanol (Aasberg-Petersen et al., 2007).



### 2.1.2. Methanol Synthesis from Coal and Bio-mass gasification

The rote of production methanol from coal and biomass is similar to that for the productions of methanol from natural gas, and is subdivide into the three steps: syngas production, synthesis of crude methanol, and purification. In the first step, coal or biomass is converted inside a gasifier into gaseous products, which consist of biogas (CH<sub>4</sub> and CO<sub>2</sub>), syngas (H<sub>2</sub>, CO<sub>2</sub>, and CO), pure hydrogen, and alkaline gases (Dalena et al., 2018b).

According with Struis et al., 1996, methanol production form syngas utilizing conventional gasification of biomass, require higher temperatures (800 – 1000 °C); for any resource containing carbon, such as coal or solid wastes.

Moreover, biomass conversion into the gaseous product involves many reactions. Shahbaz et al., 2017, represented by equation 2 and 4, above (WGS and Steam methane reforming), and other equation are below:

- Char gasification



- Boudouard reaction



- Methanation Reaction



The effects of reactor temperature and equivalent ratio air and oxygen as gasifying agents were studied by Shahbaz et al., 2017. Therefore, the reactor temperature is one of the most important thing variables for biomass gasification. In this the reactor temperatures are varied from 1073 to 1223 K in 50 K increments. The high temperature is favorable for forward water gas shift reaction and high amount of steam increase hydrogen production and reduce CO<sub>2</sub> formation (Gao et al., 2012; Shahbaz et al., 2017). Meanwhile, the ratio of reaction is crucial factor that affects the performance of the gasification process (N. Gao et al., 2012).

Although, the synthesis gas for methanol production should only contain a small proportion of inert gas components. In fact, the use of air as a gasification agent results in a syngas with a high nitrogen content. For methanol synthesis the optimal H<sub>2</sub>:CO<sub>2</sub> ratio in the syngas is >2 and then gasification of biomass always results in a gas with a too low H<sub>2</sub>: CO<sub>2</sub> ratio. Usually the WGS process is the most frequently used process for ensuring a suitable of CO<sub>2</sub>:CO:H<sub>2</sub> and mainly to convert the co into CO<sub>2</sub> (Struis et al., 1996). The WGS reaction is exothermic reaction, is suitable at low temperature, and low pressure. The carbon monoxide is converted to carbon dioxide and hydrogen. In other hands, the carbon dioxide produced during the WGS process must be separated from the syngas in order to ensure a suitable ratio of CO<sub>2</sub>:CO:H<sub>2</sub> for the commercially available methanol production catalyst required to be 5:28:63 (Trop et al., 2014).

### 2.1.3. Methanol from catalytic hydrogenation of CO<sub>2</sub>

The carbon-oxygen bonds are very strong, and high energy is required for breaking them. For this reason, in order to convert CO<sub>2</sub> into methanol, a good catalytic system is required (Dalena et al.,

2018b). Then, the chemical reduction of CO<sub>2</sub> can be categorized into two groups: heterogeneous reduction and homogeneous reduction. The heterogeneous catalysis is technically more favorable, in relation with the stability, separation, handling reuse of the catalysts and reactor design (Zangeneh et al., 2011).

Therefore, industrial methanol production from CO<sub>2</sub>-containing syngas uses the well-known Cu-ZnO-Al<sub>2</sub>O<sub>3</sub> catalysts. Currently, CH<sub>3</sub>OH synthesis from catalytic CO<sub>2</sub> hydrogenation has been implemented at the pilot-plant level by Lurgi, Mitsui, CRI, among others. The process mainly used modified Cu-ZnO-Al<sub>2</sub>O<sub>3</sub>, Cu-ZrO<sub>2</sub>, and Cu-ZnO-ZrO<sub>2</sub> catalysts and were carried out under conditions supported copper materials have attracted much attention to CH<sub>3</sub>OH, due to the low cost, high activity, and selectivity associated with Cu to produce methanol. The conventional Cu-ZnO methanol synthesis catalysts exhibit low activity in hydrogenation of both pure CO and CO<sub>2</sub> to methanol. (P. Gao et al., 2020; Nguyen & Zondervan, 2019; Marcos et al., 2022). In other hands, the low activity of the catalyst in CO<sub>2</sub> and CO hydrogenation is affected by RWGS, this reaction accelerates the crystallization of Cu and ZnO in the catalyst, leading to the deactivation the catalyst by sintering. To prevent this situation, addition of small amount of silica into the catalyst greatly improves the catalyst stability by suppressing the crystallization of Cu and ZnO (Nguyen & Zondervan, 2019).

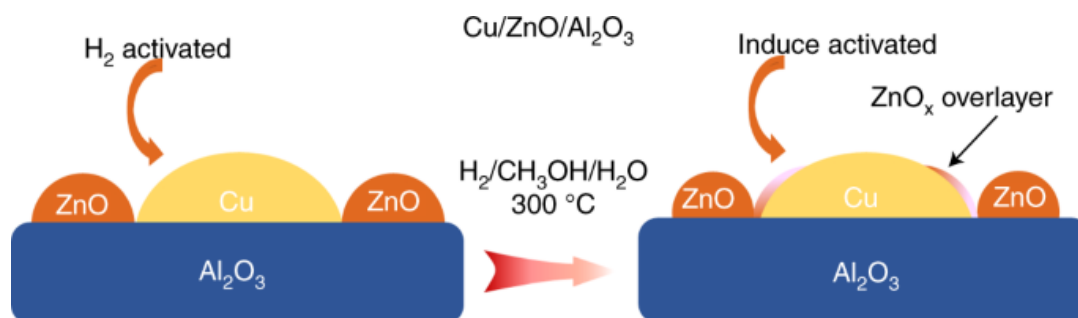


**Figure 1:** Methanol Production based on Cu-ZnO-Al<sub>2</sub>O<sub>3</sub> catalyst (Li et al., 2022).

## 2.2. Methanol Kinetics Model

According to Izbassarov et al., 2022; and Poto et al., 2022, in any catalytic process, kinetic modelling is an essential tool to support efforts on catalyst development, to elucidate reaction mechanisms as well as to avoid reactor design and process optimization. However, numerous kinetic models have been proposed over the years to describe the methanol synthesis, mostly on

commercial catalyst. The kinetic model described by Graaf & Stamhuis, 1988, was addressed for low pressure methanol synthesis applying the commercial catalyst (CuO-ZnO-Al<sub>2</sub>O<sub>3</sub>) and methanol synthesis kinetics described according Langmuir-Hinshelwood (LHHW) mechanism, carried on between 210 – 245 °C and 15 to 50 bar, based on dissociative hydrogen adsorption and three independent reactions: methanol formation from CO<sub>2</sub>, methanol formation from CO, and the WGS reaction. And, Bussche & Froment, 1996, model describe effect of inlet temperature and pressure. At low inlet temperature, around 180 °C, the model predicts a very limited hydrogenation activity, observed in isothermal experiments condition. At 200 °C, observed that both reactions proceed at higher rate, and consequently the RWGS changes direction earlier in the bed, varying the inlet pressure, and table 1 show the different kinetic models.

Therefore, Vander Bussche-Froment and Gaaf models are the ancestors of all the kinetic models summarized on table 1, and Bisotti et al., 2022, Izbassarov et al., 2022, discussed in their report of the different performance of modified or refitted model of VBF and Gaaf model. The resulting refitted kinetics are appreciable, example Nestler et al., 2020 and Henkel, 2011 their refitted models is appreciable and respectively, their models are more accurate and reliable compared to the original ones. The Nestler et al., 2020, reported that, reason behind the accurate is, the reaction rate constants for CO<sub>2</sub> hydrogenation and RWGS increase with increase temperature. And, while the adsorptions constants for CO as well as H<sub>2</sub>O and H<sub>2</sub> decrease with increasing temperature, the adsorption constant for CO<sub>2</sub> not presented any temperature dependence. In other hands, advanced that, special caution should be taken when applying the proposed model for description of modern methanol synthesis reactors. As water has a strongly inhibition effect on the kinetics of methanol synthesis, measurements with high CO<sub>2</sub> contents should be included into kinetic measurement campaigns especially with regard to power-to-methanol (PtM) application. Exclusion of high CO<sub>2</sub> contents from the kinetic measurement could lead towards an overestimated model activity as shown with the kinetic model proposed by Henkel, 2011.



**Table 1:** The commonly kinetic model and recently proposed model

Model	Carbon		Parameters (T, P)	Reactions	Notes
	source				
Graaf & Stamhuis, 1988	CO		P (30 – 50 bar)	$\text{CO}_2 + 3\text{H}_2 \Rightarrow \text{CH}_3\text{OH} + \text{H}_2\text{O}$	Completes schems
	and		T > 245 °C	$\text{CO}_2 + \text{H}_2 \Rightarrow \text{CO} + \text{H}_2\text{O}$	
	CO <sub>2</sub>			$\text{CO} + 2\text{H}_2 \Rightarrow \text{CH}_3\text{OH}$	
Bussche & Froment, 1996			P (15 – 51 bar)		
			T (180 – 280 °C)		
	CO <sub>2</sub>		P (50 – 80 bar)	$\text{CO}_2 + 3\text{H}_2 \Rightarrow \text{CH}_3\text{OH} + \text{H}_2\text{O}$	CO direct hydrogenation is removed
Nestler et al., 2020			T < 270 °C	$\text{CO}_2 + \text{H}_2 \Rightarrow \text{CO} + \text{H}_2\text{O}$	
	CO <sub>2</sub>			$\text{CO}_2 + 3\text{H}_2 \Rightarrow \text{CH}_3\text{OH} + \text{H}_2\text{O}$	Completes schems
Bisotti et al., 2021	And			$\text{CO}_2 + \text{H}_2 \Rightarrow \text{CO} + \text{H}_2\text{O}$	
	CO			$\text{CO} + 2\text{H}_2 \Rightarrow \text{CH}_3\text{OH}$	

### 2.3. Commercial Technology for methanol Synthesis

The methanol rate of production and thermodynamic limitations are a direct consequence of the kinetics. And Several papers analyzed different industrial technologies highlighting their advantages and the disadvantages of the competitors. Many of these works show that the main target during reactor design is to guarantee the optimal temperature profile, thus minimizing as much as possible the reactor volume (Bisotti et al., 2022).

In the present work, we present a brief highlight of the main currently adopted technological solutions.

#### 2.3.1. High to low Pressure methanol synthesis

The first technology, commercialized by BASF in 1923, was based on a ZnO-Cr<sub>2</sub>O<sub>3</sub> catalyst that could hydrogenate CO to methanol at 240 – 300 bar and 350 – 400 °C. The process use the ZnO-Cr<sub>2</sub>O<sub>3</sub> o avoid high temperature (exothermic reaction), cold gas is injected in the catalyst bed. This catalyst also produced methane and other light hydrocarbons with 2 – 5 wt. % selectivity. Then, production of methanol with ZnO-Cr<sub>2</sub>O<sub>3</sub> catalysts by the high-pressure process is no longer economical. The last methanol plant based on this process closed in the mid-1980s (Lange, 2001; OTT et al., 2012).

A major improvement wt. % achieved in the 1960s by producing a Sulphur-free synthesis gas that enabled ICI to use the more active Cu/ZnO catalyst, applying an adiabatic reactor with a single catalyst bed. The reaction is quenched by adding cold reactant gas at different heights in the catalyst bed. Due the high activity, this catalyst could operate at much low pressure and temperature, namely 60 – 80 bar and 250 – 280 °C. These improvements resulted in a significant reduction of the compression and heat exchange duty in the recycle loop (Moulijn et al., 2013; Lange, 2001).

The Lurgi process is very similar to the ICI process. The most important difference is the reactor. In the Lurgi process, a cooled tubular reactor is used, showed in (figure 2). The lurgi rector is nearly isothermal. The heat of reaction is directly used or the generation high-pressure steam, which is used to drive the compressors and, subsequently, as distillation steam. While, in the Haldor Topsoe process, several adiabatic reactors are use, arranged in series. Intermediate coolers remove the heat of reaction. The syngas flows radially through the catalyst beds, which results in reduced pressure drop compared to axial flow (Palma et al., 2018; Moulijn et al., 2013).

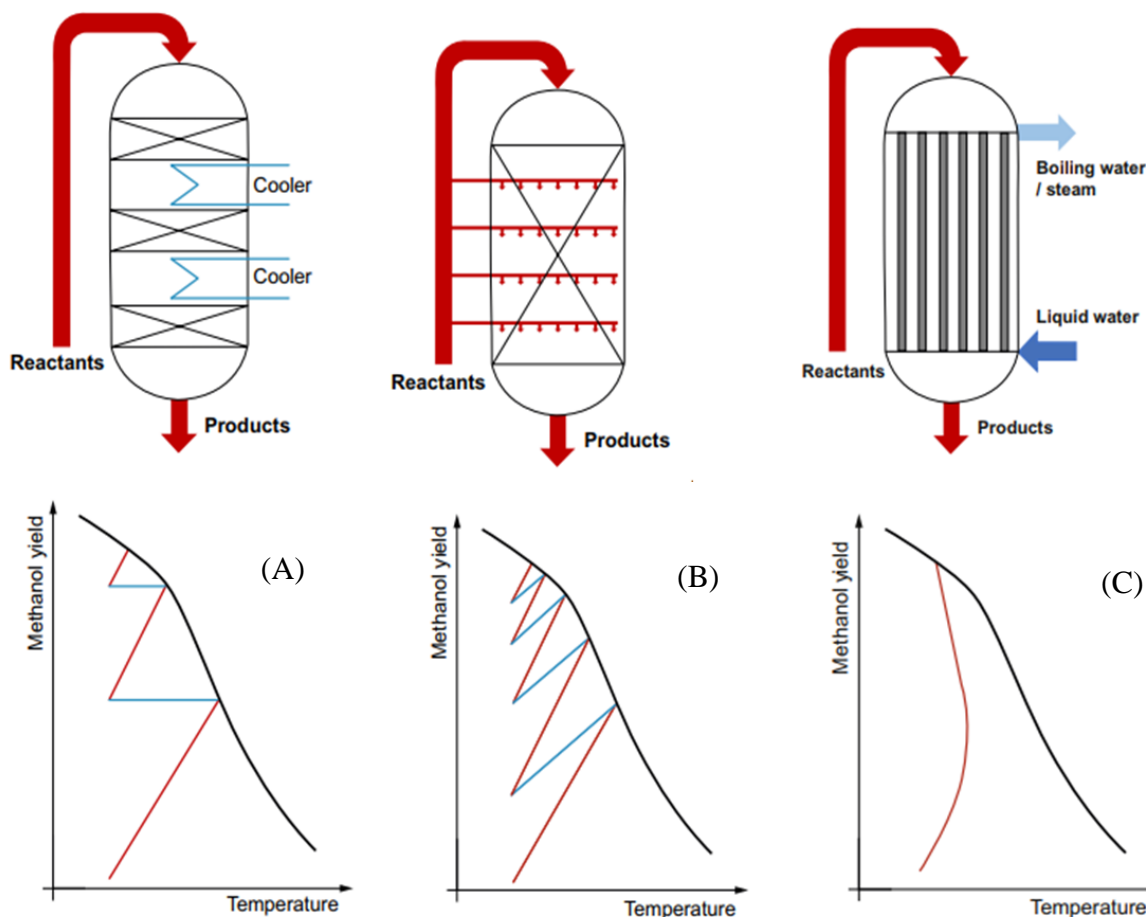


**Figure 2:** Temperature profile of the commercial methanol technologies: (A) direct quenching (ICI), (B) indirect cooling (Haldor Topsoe), and (C) quasi-isothermal BWR (Lurgi) (Bisotti et al., 2022).

Therefore, the quench reactor (figure 2-A). It is one of the simplest systems for methanol synthesis, in which only a portion of the reactants are preheated and fed into the top of the reactor, which will then be converted, thus increasing the system's temperature. While quasi-isothermal reactor (figure 2-C) employs a tubular reactor with cooling by boiling water. The catalyst is located in tubes that are surrounded by boiling water for heat of reaction removal. The temperature of the cooling medium is adjusted by a preset pressure in the steam drum (Ott et al., 2012; Palma et al., 2018; Bisotti et al., 2022).

## CHAPTER 3 – METHODOLOGIES

### 3.1. Overview

This chapter describes the methodologies employed to achieve the aim of this study, which focuses on the comparative analysis and economic evaluation of methanol production from CO<sub>2</sub> hydrogenation using different kinetic models. The following steps were undertaken:

- Literature review: a comprehensive review of existing literature was conducted to gather information on various kinetic models reported in previous studies. This review aimed to identify and compare the different approaches to methanol synthesis via CO<sub>2</sub> hydrogenation.
- ASPEN HYSYS Simulations: The Aspen Hysys V11 software was used to develop simulations for the different kinetic models. The following steps were followed in the simulation process:
  - a) Properties package: The Peng-Robinson properties package was selected for the simulations.
  - b) Kinetic model fit: different kinetic models were fitted to simulation data, such as original Graaf and Farm (GF) model, Vanden Bussche and Fromen (VBF) model, and two schemes Graaf model.
  - c) Reactor model design: The design of a Plug Flow Reactor (PFR) was developed and detailed in the next chapter
  - d) Heat exchanger (HE), compressor and cooler Design: were incorporated into the simulation to manager thermal energy transfer.
- Distillation Column (DC) Design: Distillation columns were designed to further purify the methanol product.
- Kinetics model validation: The kinetics models were validated against literature data to ensure their accuracy and reliability.
- Results and discussion: the results of the simulations were analyzed and discussed, focusing on the performance and economic viability of each kinetic model for methanol production.
- Conclusion and recommendations: The concluded with a summary of finding and recommendations for future research and industrial application.

### 3.1.1. Kinetic models schemes

In this paper, four kinetic models (KM) are compared, each other, based in two commonly used models in process simulation presented or discussed in previous studies, the original Graaf et al., 1988 and the VF model as presented by Vanden & Froment, 1996, and compare with refitted Graaf model as presented by Bisotti et al., 2021, and also the GR model excluding the CO hydrogenation introduced in this work. These models have been selected due to being either commonly used or recently developed and are the most consolidate an adopted model in industrial practice. Moreover, all the considered models are developed for commercial Cu-based catalysts and consider either only CO<sub>2</sub> hydrogenation or the hydrogenation of both CO and CO<sub>2</sub> including the RWGS reaction. And the further step it is presented or discussion the rate equation of each KMs, table below show the kinetic parameter.

#### a) Vander and Froment Model

$$R_{CH_3OH} (kmol/(kg_{cat} \cdot s)) = \frac{k_1 p_{CO_2} p_{H_2} \left(1 - \frac{1}{K_{eq1}} \frac{p_{H_2O} p_{CH_3OH}}{p_{H_2}^3 p_{CO_2}}\right)}{\left(1 + K_2 \frac{p_{H_2O}}{p_{H_2}} + K_3 \sqrt{p_{H_2}} + K_4 p_{H_2O}\right)^3} \rho_{cat} (1 - \psi) \quad (10)$$

$$R_{RWGS} (kmol/(kg_{cat} \cdot s)) = \frac{k_1 p_{CO_2} \left(1 - \frac{1}{K_{eq1}} \frac{p_{H_2O} p_{CO}}{p_{H_2} p_{CO_2}}\right)}{\left(1 + K_2 \frac{p_{H_2O}}{p_{H_2}} + K_3 \sqrt{p_{H_2}} + K_4 p_{H_2O}\right)^1} \rho_{cat} (1 - \psi) \quad (11)$$

#### b) Original and refitted Graaf model

$$R_{CH_3OH/CO_2} (kmol/(kg_{cat} \cdot s)) = \frac{k_1 K_{CO_2} \left(p_{CO_2} p_{H_2}^{1.5} - \frac{1}{K_{eqCO_2}} \frac{p_{H_2O} p_{CH_3OH}}{p_{H_2}^{1.5}}\right)}{\left(1 + K_{CO} p_{CO} + K_{CO_2} p_{CO_2}\right) \left(p_{H_2}^{1.5} + \frac{K_{H_2O}}{K^{0.5}} p_{H_2O}\right)} \rho_{cat} (1 - \psi) \quad (12)$$

$$R_{RWGS} (kmol/(kg_{cat} \cdot s)) = \frac{k_1 K_{CO_2} \left(p_{CO_2} p_{H_2} - \frac{1}{K_{eqRWGS}} \frac{p_{CH_3OH} p_{CO}}{p_{H_2}}\right)}{\left(1 + K_{CO} p_{CO} + K_{CO_2} p_{CO_2}\right) \left(p_{H_2}^{1.5} + \frac{K_{H_2O}}{K^{0.5}} p_{H_2O}\right)} \rho_{cat} (1 - \psi) \quad (13)$$

$$R_{CH_3OH/CO} (kmol/(kg_{cat} \cdot s)) = \frac{k_1 K_{CO} \left(p_{CO} p_{H_2}^{1.5} - \frac{1}{K_{eqCO_2}} \frac{p_{CH_3OH}}{p_{H_2}^{0.5}}\right)}{\left(1 + K_{CO} p_{CO} + K_{CO_2} p_{CO_2}\right) \left(p_{H_2}^{1.5} + \frac{K_{H_2O}}{K^{0.5}} p_{H_2O}\right)} \rho_{cat} (1 - \psi) \quad (14)$$

#### c) Nestle model

$$\frac{R_{CH_3OH}}{CO_2} (kmol/(kg_{cat} \cdot s)) = \frac{k_1 K_{CO_2} \left(p_{CO_2} p_{H_2}^{1.5} - \frac{1}{K_{eqCO_2}} \frac{p_{H_2O} p_{CH_3OH}}{p_{H_2}^{1.5}}\right)}{\left(1 + K_{CO} p_{CO} + K_{CO_2} p_{CO_2}\right) \left(p_{H_2}^{1.5} + \frac{K_{H_2O}}{K^{0.5}} p_{H_2O}\right)} \rho_{cat} (1 - \psi) \quad (15)$$

$$R_{RWGS} (kmol/(kg_{cat} \cdot s)) = \frac{k_1 K_{CO_2} \left(p_{CO_2} p_{H_2} - \frac{1}{K_{eqRWGS}} \frac{p_{CH_3OH} p_{CO}}{p_{H_2}}\right)}{\left(1 + K_{CO} p_{CO} + K_{CO_2} p_{CO_2}\right) \left(p_{H_2}^{1.5} + \frac{K_{H_2O}}{K^{0.5}} p_{H_2O}\right)} \rho_{cat} (1 - \psi) \quad (16)$$

**Table 2:** The original kinetic and thermodynamic parameters for the considered kinetics,

Parameters	Or-Graaf	Ref-Graaf	VDF	F. Nestler
	Ea(J/mol), P(bar)	Ea(J/mol), P(bar)	Ea(J/mol), P(bar)	Ea(J/mol), P(Pa)
<b>Kinetics coefficient</b>	$k_1 = 1.09 * 10^5 * EXP\left(\frac{-87500}{RT}\right)$	$k_1 = 9.205 * 10^1 * EXP\left(\frac{-45889}{RT}\right)$	$k_1 = 1.07 * 10^1 * EXP\left(\frac{-36696}{RT}\right)$	$k_1 = 5.41 * 10^{-4} * EXP\left(\frac{-45458}{RT}\right)$
	$k_2 = 9.64 * 10^{11} * EXP\left(\frac{-152900}{RT}\right)$	$k_2 = 4.241 * 10^{13} * EXP\left(\frac{-149856}{RT}\right)$	$k_2 = 1.22 * 10^{10} * EXP\left(\frac{94765}{RT}\right)$	$k_2 = 24.701 * EXP\left(\frac{-54970}{RT}\right)$
	$k_2 = 4.89 * 10^7 * EXP\left(\frac{-11300}{RT}\right)$	$k_3 = 2.240 * 10^7 * EXP\left(\frac{-106729}{RT}\right)$	-	-
<b>Adsorption constant</b>	$K_{CO_2} = 7.05 * 10^{-7} * EXP\left(\frac{617000}{RT}\right)$	$K_{CO_2} = 8.206 * 10^{-9} * EXP\left(\frac{76594}{RT}\right)$	$K_1 = 3.45 * 10^3$	$K_{CO_2} = 8.262 * 10^{-6}$
	$K_{CO} = 2.16 * 10^{-5} * EXP\left(\frac{468000}{RT}\right)$	$K_{CO} = 1.540 * 10^{-3} * EXP\left(\frac{14936}{RT}\right)$	$\sqrt{K_2} = 4.99 * 10^{-1} * EXP\left(\frac{17197}{RT}\right)$	$K_{CO_2} = 3.321 * 10^{-18} * EXP\left(\frac{109959}{RT}\right)$
	$\frac{K_{H_2O}}{K^{0.5}_{H_2}} = 6.37 * 10^{-9} * EXP\left(\frac{84000}{RT}\right)$	$K_{CO} = 3.818 * 10^{-9} * EXP\left(\frac{97350}{RT}\right)$	$K_3 = 6.62 * 10^{-11} * EXP\left(\frac{124119}{RT}\right)$	$\frac{K_{H_2O}}{K^{0.5}_{H_2}} = 6.430 * 10^{-14} * EXP\left(\frac{119570}{RT}\right)$
<b>Equilibrium constant</b>	$\log_{10} K_{eq,CO_2} = \frac{3066}{T} - 10.592$		$\log_{10} K_{eq,CO_2} = \frac{3066}{T} - 10.592$	
	$\log_{10} K_{eq,RWGS} = -\frac{2073}{T} - 2.592$		$\log_{10} K_{eq,RWGS} = -\frac{2073}{T} - 2.592$	
	$\log_{10} K_{eq,CO_2} = \frac{5139}{T} - 12.621$			

Source: Bisotti et al., (2022); Nestler et al., (2020). Activation energy are expressed in kj/kmol\*, and the pressure are in bar for Graaf and VDF model, for Nestler the pressure is in Pa.

### 3.1.1.1. Rearrangement of the kinetic rate

The rate equation (13,14 and 15) above should be reformulated or rewrite, because the Aspen HYSYS suite requires a specific parametric formula for the reaction rates, to be compliant with the software requirements. This general form follows the structure of Langmuir-Hinshelwood-Hougen-Watson (LHHW) type kinetics. The general rate in aspen Hysys (Aspentech, 2005):

$$R = \frac{k_{dir} * p_i - k_{rec} * p_i}{(1 + \sum_{i=1}^N K_i p_i)^n} \quad (17)$$

Where,

- $k_{dir}$  and  $k_{rev}$  are the kinetic constants of the direct and reverse reaction, respectively, and
- $K_i$  is the adsorption parameters appearing in the denominator.

The terms at the numerator  $p_{(direct)}$  and  $P_{i (rev)}$  are functions of the species pressure. The kinetic constant and the adsorption parameters are defined according to the conventional Arrhenius law.

$$k_i = A_i * EXP\left(-\frac{E_i}{RT}\right) \quad (18)$$

$$K_j = A_j * EXP\left(-\frac{E_j}{RT}\right) \quad (19)$$

Now, firstly should be rearrange the numerator (NT) of each rate equation. Starting with the rate equation (10 and 11).

$$NT = k_1 p_{CO_2} p_{H_2} \left(1 - \frac{1}{K_{eq1}} \frac{p_{H_2O} p_{CH_3OH}}{p_{H_2}^3 p_{CO_2}}\right) \quad (20)$$

After expanded the:

$$NT = k_1 p_{CO_2} p_{H_2} - \frac{k_1}{K_{eq1}} \frac{p_{H_2O} p_{CH_3OH}}{p_{H_2}^2} \quad (21)$$

The numerate of rate (11):

$$NT = k_1 p_{CO_2} \left(1 - \frac{1}{K_{eq1}} \frac{p_{H_2O} p_{CO}}{p_{H_2} p_{CO_2}}\right) \quad (22)$$

After expanded:

$$NT = k_1 p_{CO_2} - \frac{k_1}{K_{eq1}} \frac{p_{H_2O} p_{CO}}{p_{H_2}} \quad (23)$$

Therefore, the denominator of this two rate equation it is not necessary an arrangement because it is represented as LHHW.

Rearrangement of the rate equation (24, 25 and 26):

$$NT = k_1 K_{CO_2} \left( p_{CO_2} p_{H_2}^{1.5} - \frac{1}{K_{eqCO_2}} \frac{p_{H_2O} p_{CH_3OH}}{p_{H_2}^{1.5}} \right) \quad (24)$$

After expanded:

$$NT = k_1 K_{CO_2} p_{CO_2} p_{H_2}^{1.5} - \frac{k_1 K_{CO_2}}{K_{eqCO_2}} \frac{p_{H_2O} p_{CH_3OH}}{p_{H_2}^{1.5}} \quad (25)$$

$$NT = k_1 K_{CO_2} \left( p_{CO_2} p_{H_2} - \frac{1}{K_{eqRWGS}} p_{CH_3OH} p_{CO} \right) \quad (26)$$

$$NT = k_1 K_{CO_2} p_{CO_2} p_{H_2} - \frac{k_1 K_{CO_2}}{K_{eqRWGS}} p_{CH_3OH} p_{CO} \quad (27)$$

$$NT = k_1 K_{CO} \left( p_{CO} p_{H_2}^{1.5} - \frac{1}{K_{eqCO_2}} \frac{p_{CH_3OH}}{p_{H_2}^{0.5}} \right) \quad (28)$$

$$NT = k_1 K_{CO} p_{CO} p_{H_2}^{1.5} - \frac{k_1 K_{CO}}{K_{eqCO_2}} \frac{p_{CH_3OH}}{p_{H_2}^{0.5}} \quad (29)$$

And assume that denominator (DEN) of the rate equation is represented as follow bellow:

$$EN = \left( 1 + K_{CO} p_{CO} + K_{CO_2} p_{CO_2} \right) \left( p_{H_2}^{1.5} + \frac{K_{H_2O}}{K_{H_2}^{0.5}} p_{H_2O} \right) \quad (30)$$

$$DEN = \left( p_{H_2}^{1.5} + \frac{K_{H_2O}}{K_{H_2}^{0.5}} p_{H_2O} + K_{CO} p_{CO} p_{H_2}^{1.5} + K_{CO} p_{CO} \frac{K_{H_2O}}{K_{H_2}^{0.5}} p_{H_2O} \right. \\ \left. + K_{CO_2} p_{CO_2} p_{H_2}^{1.5} + K_{CO_2} p_{CO_2} \frac{K_{H_2O}}{K_{H_2}^{0.5}} p_{H_2O} \right) \quad (31)$$

Then, aggrupation the commonly factor

(32)

Several terms of the kinetic adsorption equations were omitted for simplification assuming that the change of  $p_{H_2}^{1.5}$  is small and factorizing this term, the equation will be:



$$DEN = \left( p_{H_2}^{1.5} \left( 1 + K_{CO} p_{CO} + \frac{K_{H_2O}}{K^{0.5}_{H_2}} \frac{p_{H_2O}}{p_{H_2}^{1.5}} + K_{CO} p_{CO} \frac{K_{H_2O}}{K^{0.5}_{H_2}} \frac{p_{H_2O}}{p_{H_2}^{1.5}} \right) + \left( K_{CO_2} p_{CO_2} p_{H_2}^{1.5} + K_{CO_2} p_{CO_2} \frac{K_{H_2O}}{K^{0.5}_{H_2}} p_{H_2O} \right) \right) \quad (33)$$

And it is notable existence of relationship between  $p_{H_2}^{1.5}$  and  $p_{H_2O}$ , it notable that the  $p_{H_2}^{1.5} \gg p_{H_2O}$ , and the ration between  $\frac{p_{H_2O}}{p_{H_2}^{1.5}} \ll 1$ , other hand, the value it can be across to zero. It is means some terms in adsorption equation are neglected, such as  $\frac{K_{H_2O}}{K^{0.5}_{H_2}} \frac{p_{H_2O}}{p_{H_2}^{1.5}}$  an.  $K_{CO} p_{CO} \frac{K_{H_2O}}{K^{0.5}_{H_2}} \frac{p_{H_2O}}{p_{H_2}^{1.5}}$

The equation become:

$$DEN = \left( p_{H_2}^{1.5} (1 + K_{CO} p_{CO}) + \left( K_{CO_2} p_{CO_2} p_{H_2}^{1.5} + K_{CO_2} p_{CO_2} \frac{K_{H_2O}}{K^{0.5}_{H_2}} p_{H_2O} \right) \right) \quad (34)$$

If assume that  $p_{H_2}^{1.5} (1 + K_{CO} p_{CO})$  is a function of  $F(p) = p_{H_2}^{1.5} (1 + K_{CO} p_{CO})$ , and it is notable that the  $p_{H_2}^{1.5} (1 + K_{CO} p_{CO}) \approx p_{H_2}^{1.5}$ . And the effect of  $p_{H_2}^{1.5}$  can affect the  $(1 + K_{CO} p_{CO})$  term theoreticaly in domine  $(0 - 1)$ .

If the  $p_{H_2}^{1.5} = 1$ , it can notable the maxim effect on CO adsorption term, and replace it in equation we can get.

$$DEN = \left( (1 + K_{CO} p_{CO}) + \left( K_{CO_2} p_{CO_2} p_{H_2}^{1.5} + K_{CO_2} p_{CO_2} \frac{K_{H_2O}}{K^{0.5}_{H_2}} p_{H_2O} \right) \right) \quad (35)$$

The final equation of denominator rearranged:

$$DEN = 1 + K_{CO} p_{CO} + K_{CO_2} p_{CO_2} p_{H_2}^{1.5} + K_{CO_2} p_{CO_2} \frac{K_{H_2O}}{K^{0.5}_{H_2}} p_{H_2O} \quad (36)$$

We would remark that the proposed kinetics is based on the mass of the catalyst. Aspen HYSYS works with kinetic rate expressed per unit of reactor volume; hence, it is necessary to know the catalyst density and the void fraction within the packed bed. So, the (table 3,4 and 5) below show all summarized rate equation with their respectively Arrhenius constant.

Table 3: Reformulated reaction rate (Compliant with the Aspen HYSYS PFR reactor)

Kinetic	Reaction	Rate (kmol/(Kcats.s))
Original and ref Graaf	CO <sub>2</sub> hydrogenation	$R = \frac{k_1 K_{CO_2} p_{CO_2} p_{H_2}^{1.5} - \frac{k_1 K_{CO_2} p_{H_2O} p_{CH_3OH}}{K_{eqCO_2} p_{H_2}^{1.5}}}{1 + K_{CO} p_{CO} + K_{CO_2} p_{CO_2} p_{H_2}^{1.5} + K_{CO_2} p_{CO_2} \frac{K_{H_2O}}{K^{0.5}_{H_2}} p_{H_2O}}$
	RWGS	$R = \frac{k_1 K_{CO_2} p_{CO_2} p_{H_2} - \frac{k_1 K_{CO_2}}{K_{eqRWGS}} p_{CH_3OH} p_{CO}}{1 + K_{CO} p_{CO} + K_{CO_2} p_{CO_2} p_{H_2}^{1.5} + K_{CO_2} p_{CO_2} \frac{K_{H_2O}}{K^{0.5}_{H_2}} p_{H_2O}}$
	CO hydrogenation	$R = \frac{k_1 K_{CO} p_{CO} p_{H_2}^{1.5} - \frac{k_1 K_{CO}}{K_{eqCO_2}} \frac{p_{CH_3OH}}{p_{H_2}^{0.5}}}{1 + K_{CO} p_{CO} + K_{CO_2} p_{CO_2} p_{H_2}^{1.5} + K_{CO_2} p_{CO_2} \frac{K_{H_2O}}{K^{0.5}_{H_2}} p_{H_2O}}$
Vand-Brasslu	CO <sub>2</sub> hydrogenation	$R = \frac{k_1 p_{CO_2} p_{H_2} - \frac{k_1}{K_{eq1}} \frac{p_{H_2O} p_{CH_3OH}}{p_{H_2}^2}}{\left(1 + K_2 \frac{p_{H_2O}}{p_{H_2}} + K_3 \sqrt{p_{H_2}} + K_4 p_{H_2O}\right)^3}$
	RWGS	$R = \frac{k_1 p_{CO_2} - \frac{k_1}{K_{eq1}} \frac{p_{H_2O} p_{CO}}{p_{H_2}}}{1 + K_2 \frac{p_{H_2O}}{p_{H_2}} + K_3 \sqrt{p_{H_2}} + K_4 p_{H_2O}}$
Nestler	CO <sub>2</sub> hydrogenation	$R = \frac{k_1 K_{CO_2} p_{CO_2} p_{H_2}^{1.5} - \frac{k_1 K_{CO_2} p_{H_2O} p_{CH_3OH}}{K_{eqCO_2} p_{H_2}^{1.5}}}{1 + K_{CO} p_{CO} + K_{CO_2} p_{CO_2} p_{H_2}^{1.5} + K_{CO_2} p_{CO_2} \frac{K_{H_2O}}{K^{0.5}_{H_2}} p_{H_2O}}$
	RWGS	$R = \frac{k_1 K_{CO_2} p_{CO_2} p_{H_2} - \frac{k_1 K_{CO_2}}{K_{eqRWGS}} p_{CH_3OH} p_{CO}}{1 + K_{CO} p_{CO} + K_{CO_2} p_{CO_2} p_{H_2}^{1.5} + K_{CO_2} p_{CO_2} \frac{K_{H_2O}}{K^{0.5}_{H_2}} p_{H_2O}}$

**Table 4:** Kinetic parameters of the reformulate model (activation energy in (J/mol))

Reaction	Kinetic parameter	Or-Graaf		Ref-Graaf		VBF		Nestler	
		A	Ea	A	Ea	A	Ea	A	Ea
CO <sub>2</sub> hydrogenation	K <sub>dir</sub>	7.68E-2	2.58E4	7.55E-7	-3.07E5	1.07	-3.67E4	4.47E-10	-45458
	K <sub>rev</sub>	3.01E9	845E4	2.95E4	2.80E4	4.18E10	2.20E4	17.54	-104163.13
RWGS	K <sub>dir</sub>	6.80E5	9.12E4	3.48E5	7.33E4	1.22e10	9.48E4	2.048E-4	-54970
	K <sub>rev</sub>	6.36E3	5.15E4	3.26E3	3.36E4	1.14E8	5.51E4	1.907E-6	-51007.98
CO hydrogenation	K <sub>dir</sub>	1.06E3	6.62e4	3.45E4	9.18e4				
	K <sub>rev</sub>	4.41E15	1.65E5	1.44E17	1.90E5				

**Table 5:** Parameter of Adsorption constant-Adsorption energy in (J/mol)

Adsorption constants	Or-GR		Ref-GR		Nestler			Nestler	
	B	E <sub>ads</sub>	B	E <sub>ads</sub>	B	E <sub>ads</sub>	Adsorption constants	B	E <sub>ads</sub>
K <sub>CO</sub>	2.16E-5	-4.68E4	1.54E-3	-1.49E-4	3.321E-18	109959	K <sub>1</sub>	3.45E3	0
K <sub>CO2</sub>	7.05E-7	-6.17E4	8.21e-9	-7.66E4	8.262E-6	0	K <sub>2</sub> <sup>0.5</sup>	4.99E1	-1.72E4
K <sub>ADS*</sub>	6.37E-9	-8.40E4	3.82E-9	-9.74E4	6.430E-4	119590	K <sub>3</sub>	6.62E-11	-1.24E5
K <sub>ADS*</sub> =K <sub>CO2</sub> (K <sub>H2O</sub> /K <sup>0.5</sup> <sub>H2</sub> )									

### 3.2. Simulation process

The simulation process was carried on in aspen Hysys software V11 as mentioned before. The Peng-Robinson (PR) equation of state (EoS) is adopted to characterize the thermodynamic properties of the mixtures. We adopted the PR thermodynamic model from Hysys list (not the Aspen Properties). The component list includes CO, CO<sub>2</sub>, H<sub>2</sub>, H<sub>2</sub>O, and pure hydrogen stream. The syngas was fed in the system with 50 bar at 50 °C, and pure hydrogen 25 bar at 60 °C, respectively. Before mixed the CO<sub>2</sub> and pure hydrogen was pressurized in two stage compressor with intercooling. The pressurized feedstock is mixed with the re-pressurize recycled non-reacted gases in MIX1. Then, the mix is pre-heated in intercooler exchanger, and the goes in heat exchange model simple end point (E-103) at 200 °C, in co-current, and fed to a quasi-isothermal multi-tubular Plug Flow reactor (PFR) filled with catalyst. The products are separated after cooling in an isothermal flash separator (V-100), to liquids and non-reacted gases. The non-reacted gases are recycled to the reactor after purging in compound sprit (X-100), and pressurized in four stage compressor with intercooling, and mixed with the non-reactor gases comes in second flash separator (V-101) pressurized in five stage with intercooling.

Then, the product comes through in V-101, is pre-cooling before goes in distillation column. So, since we are tested different model, the methanol plant design was set for different condition for each kinetics model, and we can summarize all set date for simulation in the farther **table 6**.

Moreover, the plant methanol design was based on different literatures reviews, the reactor model selected was based on Lurgi technology methanol production, and simulation of the reactor sizing and setup is based on the quasi-isothermal reactor model, as which discussed by Izbassarov et al., 2022; Bisotti et al., 2022, as shows in **figure 3** below.

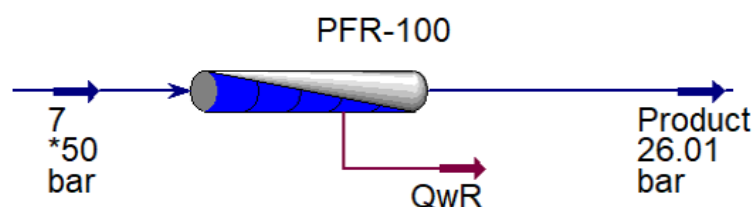


**Figure 3:** Lurgi simulation Reactor flowsheet

**Table 6:** Parameter proprieties of reactors, catalytic dimension and feed syngas composition.

Components	Molar fraction	Model			
		Or-GR	Ref-GR	VBF	Nestler
	CO <sub>2</sub>	0.0703	0.2325	0.2325	0.2325
	CO	0.2355	0.0775	0.0775	0.0775
	H <sub>2</sub>	0.6918	0.6876	0.6876	0.6876
	H <sub>2</sub> O	0.024	0.0023	0.0023	0.0023
	Pure-H <sub>2</sub>	1	1	1	1
	CH <sub>3</sub> OH	0	0	0	0
	Unit	Reactor model			
	Feed flow	Kgmol/h	40400	40640	40640
	Temperature	°C	220	220	220
	pressure	bar	60	60	30
	Number of tube	-	9000	8000	5000
	Length	m	8.7	8.7	10
Catalyst density	Kg/m <sup>3</sup>	1775	1775	1775	1775
Diameter	m	0.00375	0.00375	0.00375	0.00375
Void fraction	-	0.4	0.4	0.4	0.4
Pressure drop	bar	10	2.99		29.99
Well Heat transfer	kJ/(h-m <sup>2</sup> -C)	5.3019E5	5.965E5	5.1892E5	5.9646E5
Water cooling flow (kgmol/h)	Kgmol/h	2000	2000	2000	2000
Inlet Temperature	°C	254	254	254	254

Furthermore, the composition of syngas fed was characterized by the stoichiometric number  $S$ , given by the ratio between hydrogen and carbon dioxide moles, and the summation of the moles of CO<sub>2</sub>, and CO, as shows equation 7 below.

$$S = \frac{n(H_2) - n(CO_2)}{n(CO_2) + n(CO)} \quad (37)$$

The conversion of CO<sub>2</sub>, was calculated using (Eq.8), the conversion of H<sub>2</sub> by (Eq.9), and yield of methanol by (Eq.10) for the whole kinetic models and plant proposed in this work.

$$X_{CO_2} = \frac{n \text{ in}(CO_2) - n \text{ out}(CO_2)}{\text{moles in}(CO_2)} \quad (37)$$

$$X_{H_2} = \frac{n \text{ in}(H_2) - n \text{ out}(H_2)}{\text{moles in}(H_2)} \quad (38)$$

$$Y_{CH_3OH} = \frac{n(CH_3OH)_{prod}}{n CO_2 \text{ feed}} \quad (39)$$

$$X_{CO_2} = \frac{n \text{ in}(CO_2) - n \text{ out}(CO_2)}{\text{moles in}(CO_2)} \quad (40)$$

$$X_{H_2} = \frac{n \text{ in}(H_2) - n \text{ out}(H_2)}{\text{moles in}(H_2)} \quad (41)$$

$$Y_{CH_3OH} = \frac{n(CH_3OH),_{prod}}{n CO_2 feed} \quad (42)$$

$$Selectivity(STY) = \frac{moles\ of\ desired\ produte}{Total\ moles\ of\ desired\ products(CH_3OH + CO)} \times 100\ \% \quad (43)$$

Where,  $nCO_2$ ,  $nH_2$ ,  $nCH_3OH$  are molar flow re of  $CO_2$ ,  $H_2$ , and  $CH_3OH$  respectively. Subscript feed means the feed into the plant in streams of fuel gas feed and pure  $H_2$  feed. While moles out mean the non-reacted, purged  $CO_2$  and  $H_2$  in streams in vent, bottom and methanol.

The product leaves at the reactor, and pass through in the heat exchanger, with specific temperatures according each kinetic models. The HX, was specified with two tubes passes, one shell passes and one shell in series, in co-currents with specified pressure drops.

### 3.2.1. Crude methanol Purification

The crude methanol purification started with flesh separate V-100, to separate the light compound or volante compound non-reacted after pass through in the reactor and pre-heated, and cold, the light compound, 2 % of these is purged, and 98 % is recycled, the bottom product is fleshed through in V-101, and the light components recycled and mixed in Mix-101, and both vapors stream of V-100 and V-102, are compressed in 4 stage compressors with intercooler before re-feeding into the reactor.

The liquid from the flash tank is pumped into a 40-stage distillation column on stage 20. The column operates at 1.013 bar and the full reflux was used, so that cooling water can be used in the condenser and the water leaves in the bottom of the distillate column.

Moreover, the vapor phase constituted with higher amount of methanol, is cooled and separated in the two stage flesh tanks V-102 and V-103, to purge the remaining non-reacted gases is in pressurized at 5 and 4 stage, V-102 and V-103, with intercooler respectively, and mixed in Mix-103, and sent to the reactor.

### 3.2.2. Heat integration

In this section was based of the methodology described by Abdelaziz et al., (2017) heat integration activities and exchanger network (HEN) designs are performed on the selected process scenario based on Pinch Analysis principles and with the aid of Aspen Energy Analyzer software. This helped in maximizing energy recovery and utilization via exchanging the heat between hot and cold streams after determining the minimum heating and cooling utilities (targets).

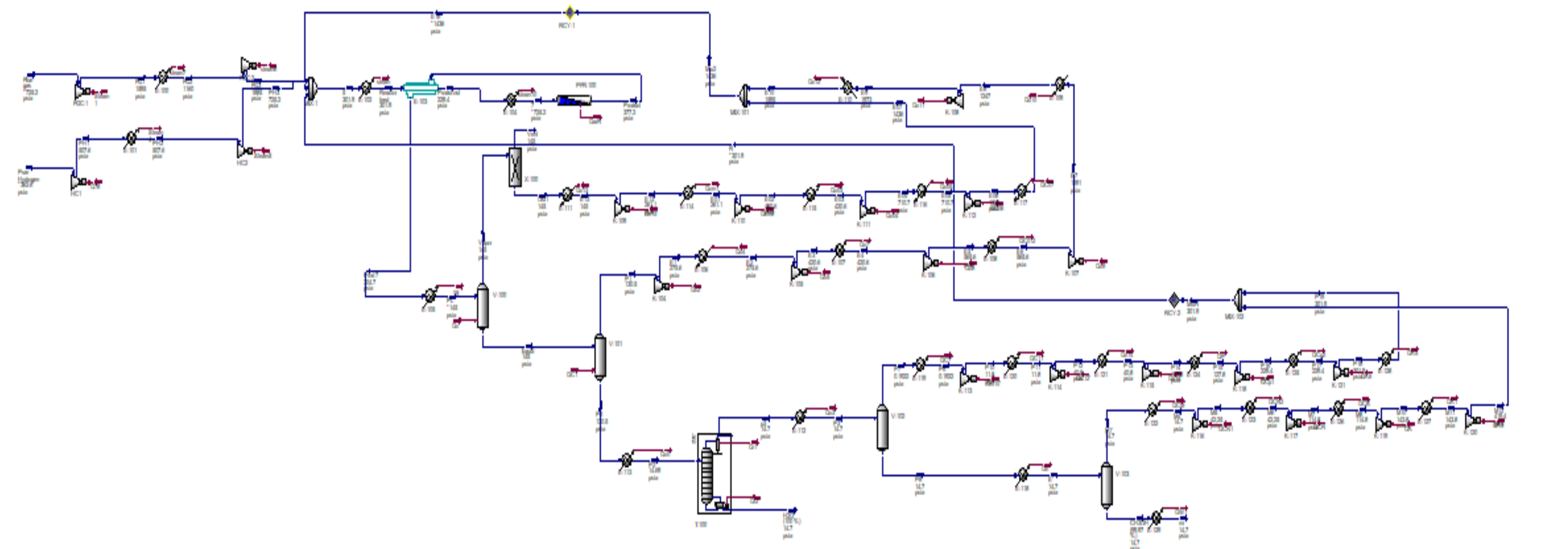


Figure 4: Process flow diagrams of proposed kinetic models for methanol Production from CO<sub>2</sub> hydrogenation.

### 3.2.3. Cost analyses

A complete economic analysis is performed for each suggested MeOH production route. Then, the cost analyses were performed with aspen economic cost estimation. Based on estimated dates, was calculated the levelized Cost of methanol (LCMeOH), following the methodologies proposed by J. Portha et al., (2021), and assumption cost parameters such as raw material (hydrogen, carbon dioxide), and catalyst as shows at table below.

Therefore, the main economical criterion considered is the Levelized Cost of methanol denoted LCMeOH, and expressed in US\$/ton) whose expression is give in **Eq. (44)** as function of the capital expenditures (CAPEX in US\$), the operational expenditures (OPEX in US\$/year), the mass flow rate of produced methanol (m MeOH in ton/year), and the Levelized life Time (LLT in year) of the process.

$$LCMeOH = \frac{\frac{CAPEX}{LLT} + OPEX}{mMeOH} \quad (44)$$

The Levelized Life Time of the process (LLT in year) is equal to 11.03 years using the following formula.

$$LLT = \frac{(1 + a)^n - 1}{a(1 + a)^{n-1}} \quad (45)$$

where n is the actual life time of the process (n = 20 years) and a is the discount rate (a = 7.4%).

The capital expenditures (CAPEX) are calculated with Eq. (46) by multiplying the purchase cost  $C_k$  of each equipment estimated by aspen in Plant cost estimate V11 and, after summing up on all equipment, by surrounding factor ( $f_e$ ). The surrounding factor considered for the plant is equal to 1.8 in this study because the plant is assumed to be implanted on an existing site.

$$CAPEX = f_e x \left( \sum_k f_k C_k \right) \quad (46)$$

The operational expenditures (OPEX) comprise two contributions as show Eq. (47):

- The variable OPEX including the purchased cost of raw materials, catalyst, and utilities as mentioned before;
- The fixed OPEX including salaries, maintenance, and management cost is equal to 3 % of the CAPEX.

$$OPEX = OPEX_{fixed} - OPEX_{var} \quad (47)$$



The variable OPEX is calculated thanks to Equation 48.

$$OPEX_{var} = P_t \times f_c \times \sum_i F_i \times UC_i \quad (48)$$

Where  $P_t$  is production time per year ( $P_t=8760$  h) and  $f_c$  is the capacity factor ( $f_c=$ ),  $F_i$  the consumption of utilities, catalyst, and raw materials (quantity/year), and  $UC_i$  the corresponding cost of each utility, catalyst, and raw materials (US\$/quantity).

According Wiesberg et al., 2016, a low-carbon low-cost of H<sub>2</sub> sought for CO<sub>2</sub> hydrogenation. Conventionally, H<sub>2</sub> is produced from fossil fuel, mainly by steam reforming of NG, accounting for 96 % of its production. Since this route is highly dependent on NG cost, H<sub>2</sub> cost can be estimated by **Eq. (49)**, which assumes methane steam reforming and partial oxidation of methane process.

$$Hydrogen\ cost\ \left(\frac{US\$}{kg}\right) = 0.286 \times NG\ price\ \left(\frac{US\$}{MMBtu}\right) + 0.15 \quad (49)$$

In spite of the recently announced Africa gas oil report, Akinosho, (2023), gas prices in Africa's domestic market have not been affected by the volatility in Europe and Asia in the last two years.

**Table 7:** Estimation prices (US\$/MMScf) of natural gas of potential African countries

Country	Prices (US\$/MMscf)
Egypt	3 – 12
Ghana	9
Nigeria	2.2
Tanzania	3
South Africa	6.5

Source: (Navarrete & Zhou, 2024, Akinosho, 2023)

Factorial estimates are based on the idea that all categories of capital expenditures in a plant are related to the cost of the purchased equipment. The equipment cost is thus evaluated through a correlation function of its main sizing parameters and is multiplied by correction factors taking into account installation and surrounding costs as well as the material type.

## CHAPTER 4 – RESULTS AND DISCUSSION

This chapter is supposed to present the most relevant results obtained and discuss how different models can influence the methanol synthesis plant. The discussions in this chapter will cover model validation, analysis of methanol yield, conversion efficiency, and selectivity of each kinetic model, crude methanol purification, heat integration and identify the most efficient and economically viable model for methanol production.

### 4.1. Sensitivity Analysis study of kinetic models

#### 4.1.1. Kinetic Model Validation

Figure 5 below shows the test of responses of different kinetic models as far as species concentration evaluation is concerned under defined operating conditions and with distinguished behavior of CO<sub>2</sub>, H<sub>2</sub>O, and CH<sub>3</sub>OH composition along the reactor length.

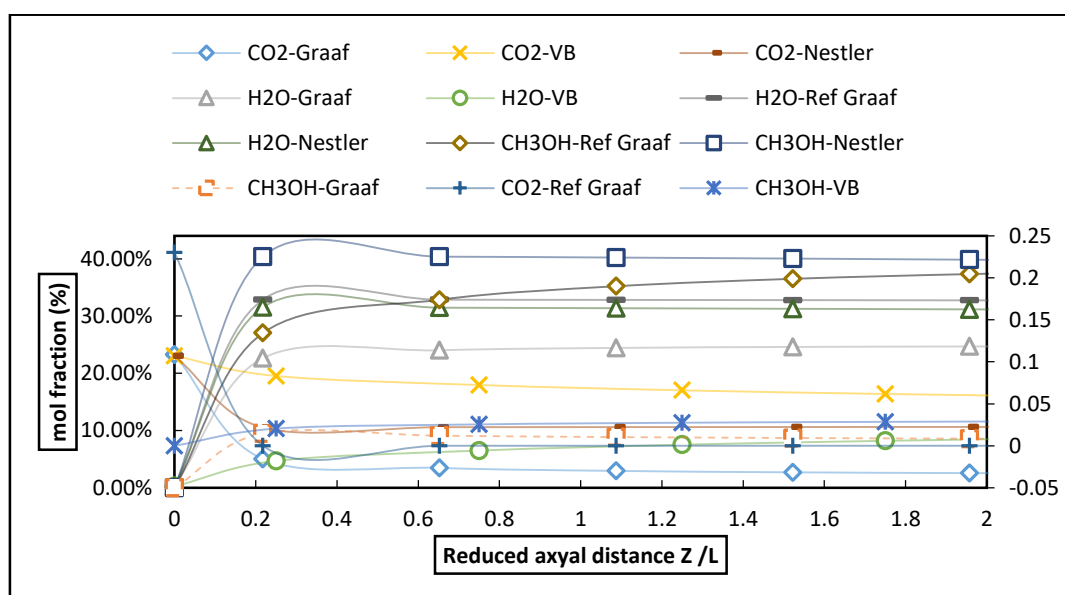


Figure 5: Simulation profile of non-adiabatic reactor of different kinetics model

The kinetics model response of CO<sub>2</sub> conversion profile is presented in figure 6 below, for four models, GAF, VB, Nestler and Ref-Graaf. The CO<sub>2</sub> consumption or conversion is great at Graaf and Ref-Graaf model, and VBF either Nestler model, have the low CO<sub>2</sub> conversion. Therefore, the different performance of CO<sub>2</sub> conversion is related with thermodynamic parameter.

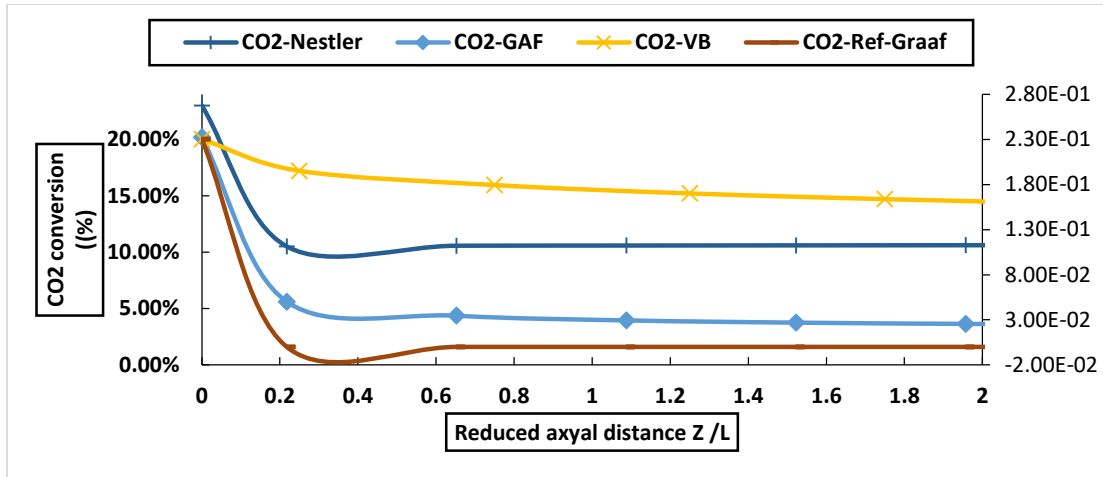


Figure 6: Simulation of CO<sub>2</sub>-conversion profile at various kinetic models

It is important to point out that in VBF models, the hydrogenation of CO<sub>2</sub> is transitioned upon by the RWGS reaction, in which the equilibrium of reaction is more dependent on temperature rather than pressure. Also, this reaction is considered mildly endothermic; therefore, it will be favored only at high temperatures, and equilibrium between the production of water and CO is reached sooner as compared to CO<sub>2</sub> hydrogenation (Nestler et al., 2020; Meyer et al., 2016). Also Tidona et al., 2013, also observed that at 50 bar and temperatures over 275, the CO<sub>2</sub> conversion becomes due to an endothermic reaction. This is indeed what has been observed in Nestler's models.

It has been reported that a higher CO<sub>2</sub> concentration reduces methanol production Lim et al., 2009, as shown in figure 7, due to the low CO<sub>2</sub> hydrogenation in the VBF model affected by RWGS. Throughout the Graaf and Nestler models, the trend can be observed that up to a maximum value of 40.40 % at a position of 0.2175 m along the reactor, the methanol production yield increases, followed by a slight reduction in yield for both models, reaching values of 36.80 % and 35.26 % after 8.4825 m of tube length. In contrast, in the Ref-Graaf model, the methanol yield continuously increases without any decreases along the reactor, while in the VBF model, methanol production does not exceed 5.0 %.

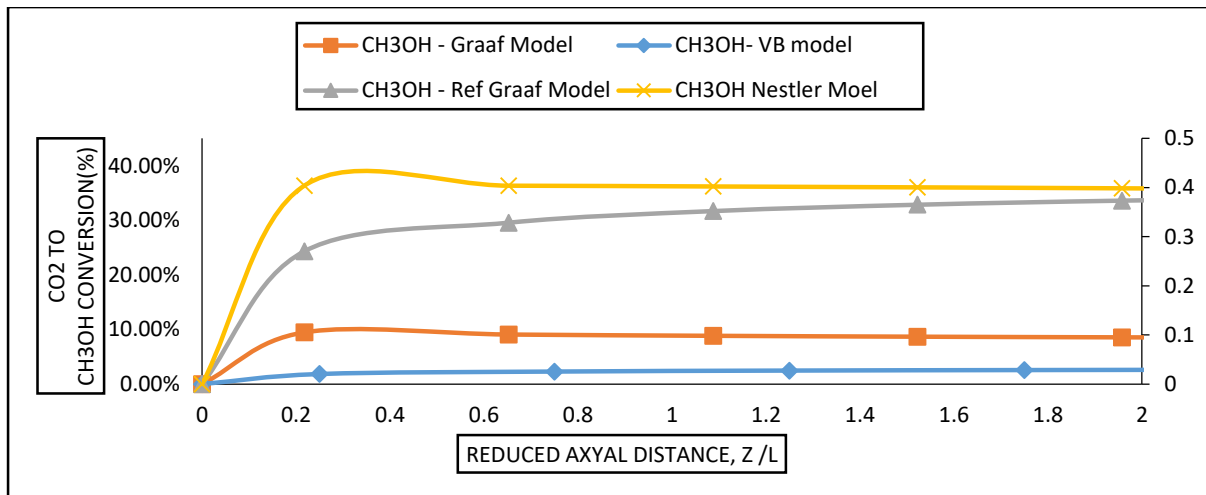


Figure 7: Simulation CH<sub>3</sub>OH yield profile of various kinetic models

Figures 8 and 9 below show the conversion of hydrogen and carbon monoxide, respectively. It could be observed from figure 7 that kinetic models developed by Nestler, Re-Graaf, and Graaf produced the highest conversions of hydrogen, at 72.92 %, 61.86 %, and 85.82 %, respectively. In contrast, the VBF model resulted in a low yield of hydrogen conversion at 35.66 %, which is due to the influence of the RWGS reaction, whose endothermic effect shifts the equilibrium to the left, increasing the concentration of the reactants. Figure 8 shows the conversion of CO<sub>2</sub> to CO. The Cui & Kær, (2019) indicated that high-temperature operation is necessary to achieve a high conversion of CO<sub>2</sub> to CO. At low temperature little CO is produced methanol in both Re-Graaf and Graaf models.

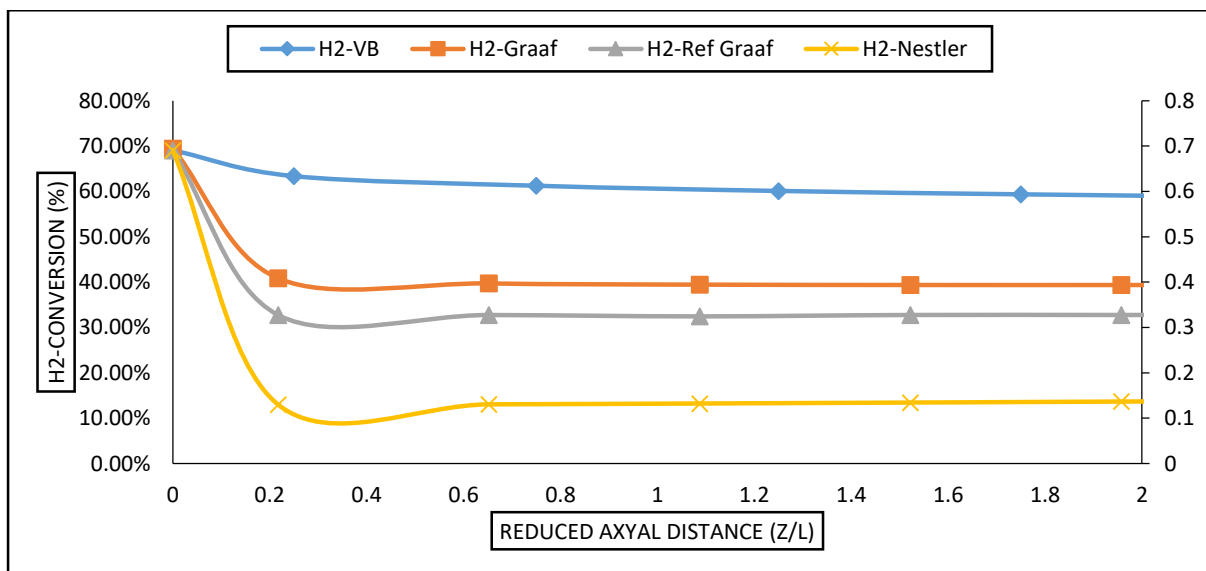


Figure 8: Simulation of H<sub>2</sub>- conversion profile of different kinetic models

Therefore, at low temperature ( $T=200 - 300\text{ }^{\circ}\text{C}$ ), little CO is produced, while CH<sub>3</sub>OH and H<sub>2</sub>O in methanol synthesis are the main products. The equilibrium composition and CO<sub>2</sub>-to-CO

conversion at these low temperatures show that the Graaf and Ref-Graaf kinetic models provide higher CO contents. However, CO<sub>2</sub> to CO conversion remains low in this temperature range for the VBF and Nestler models. At the same time, more water is produced in the system as show in figure 9.

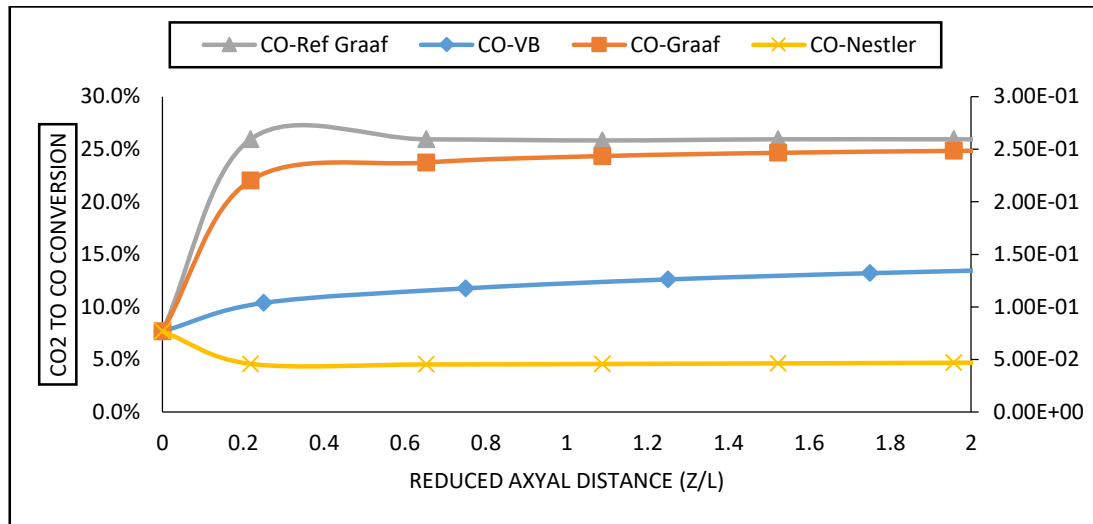


Figure 9: Simulation of CO<sub>2</sub> to CO-conversion profile of each kinetic models.

However, the by-product water can be seen in all kinetic models and is quite effective in methanol yield. Water vapor is produced in both equations 1 and 2. The inhibition of methanol formation is caused by the effect of the water produced (Marcos et al., 2022). In the Nestler and Ref-Graaf models, this is attributed to the RWGS reaction, where the equilibrium becomes favorable with increasing temperature, differing from the behavior observed in the VBF and Graaf models.

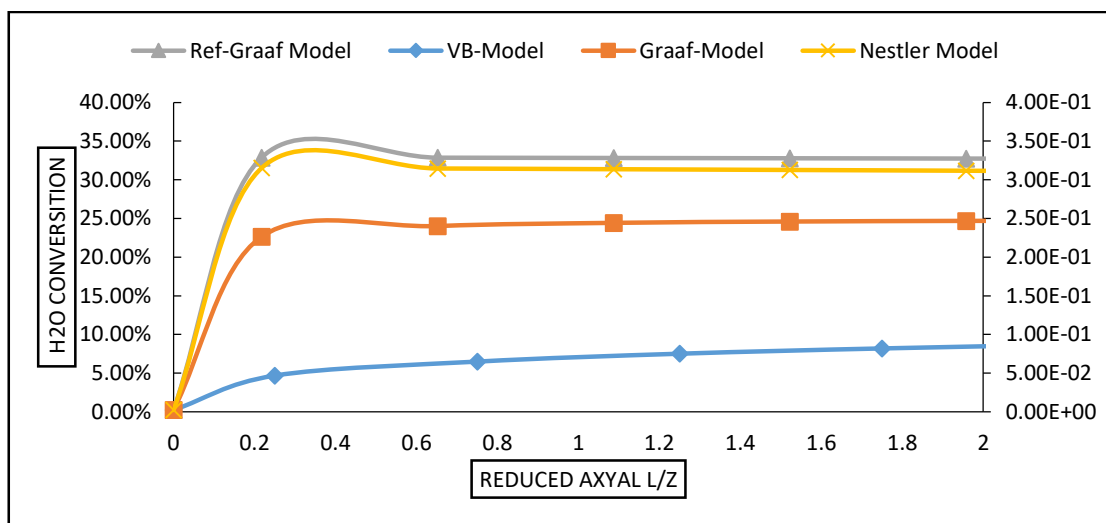


Figure 10: Simulation of H<sub>2</sub>O conversion profile of each kinetic models.

The temperature profiles show the behavior of the methanol synthesis for each kinetics model. As discussed before, temperature is one of the key factors of methanol synthesis. Figure 11 therefore gives an idea of the temperature variation for the Ref-Graaf, Graaf, VBF, and Nestler models with variation in the reactor's length while, in the case of the Nestler, Ref-Graaf, and Graaf models, the temperature increases with the rise in reactor's length. Ref-Graaf starts at a temperature of 220 °C with an increase to about 286.65 °C; Graaf starts at 220°C and increases to approximately 290.9 °C. In each model, the temperature profile is fairly flat. Nestler has a much higher starting temperature of 300 °C with a steep rise in temperature to 451.59 °C along the reactor axis. This therefore shows that the Nestler model projects a great increase in temperature along the reactor, and with this model, more heat is being generated or retained within the system. The peak temperature is reached, showing a more exothermic reaction profile.

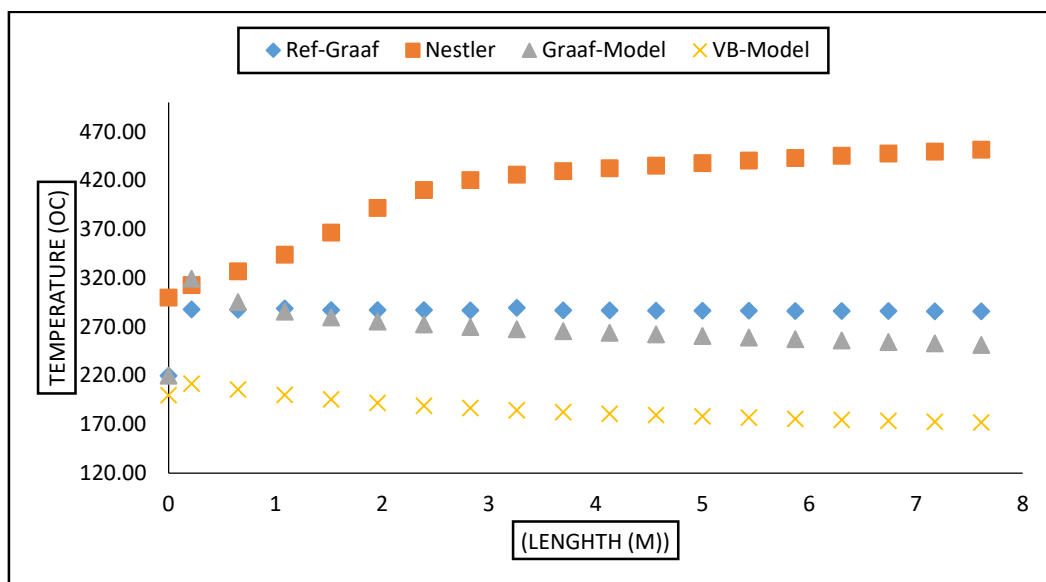


Figure 11: Temperature Profile of methanol synthesis of various kinetic models

The VBF model starts at the lowest temperature, 200 °C, and consistently shows the lowest temperatures throughout the reactor length. The temperature drops significantly to around 136.70 °C by the end. This suggests that the VBF model predicts less exothermic activity or stronger cooling effects along the reactor, which could also explain the lower methanol yield discussed earlier. The consistently lower temperature may result from the dominance of the reverse water-gas shift reaction (RWGS), which is endothermic and would pull heat out of the system. So the was observed different scenarios on the study of Cui & Kær, 2019, they got high methanol yield using BVF models using three reactor and separate for water remover. The

water removal for the RWGS process significantly improved CO<sub>2</sub>-to-CO conversion (at low operating temperatures).

#### 4.1.2. Overalls Carbon-conversion and per-pass conversion

Fresh hydrogen, carbon dioxide, and carbon monoxide were fed into the reactor using all design conditions of the different kinetic models, thermodynamic properties, and reactor packages, as shown in table 8. There are 28,070.22 kmol/h of hydrogen entering the reactor, 9,356.741 kmol/h of carbon dioxide, and 3,118.914 kmol/h of carbon monoxide. The corresponding component flow rates exiting the reactor are: for Ref-Graaf, 10,705.3 kmol/h hydrogen, 0.0003 kmol/h carbon dioxide, and 8,471.76 kmol/h carbon monoxide; for Graaf, 12355.51 kmol/h hydrogen, 868.66 kmol/h carbon dioxide, and 7993.67 kmol/h carbon monoxide; for VBF, 18,057.8 kmol/h hydrogen, 53.788 kmol/h carbon dioxide, and 6,311.71 kmol/h carbon monoxide; and for Nestler, 3,980.86 kmol/h hydrogen, 2,534.134 kmol/h carbon dioxide, and 2,764.30 kmol/h carbon monoxide. This means the overall conversions are 32.09 % for Ref-Graaf, 28.69 % for Graaf, 48.98 %, and 76.71 % for Nestler, as shown in figure 11.

**Table 8:** Composition of reactor inlet and reactor product outlets( kmols/h)

Kinetic Models	Reactor-Inlet (kmol/h)			Reactor Product Outlet (kmol/h)		
	CO <sub>2</sub>	H <sub>2</sub>	CO	CO <sub>2</sub>	H <sub>2</sub>	CO
Ref-Graaf	9356.741	28070.22	3118.914	0.0003	10705.3	8471.76
Graaf	9356.741	28070.22	3118.914	868.66	12355.51	7993.67
VBF	9356.741	28070.22	3118.914	53.788	18057.8	6311.71
Nestler	9356.741	28070.22	3118.914	2534.134	3980.86	2764.30

Thus, ref-Graaf mode shows a low overall carbon conversion, while the VBF, Graaf, and Nestler's model are high. Sometimes it is very high in terms of methanol yield, discussed previously how much possible invents can cause a reaction of feed components, and stoichiometric ratio,  $H_2/CO_2 = 3$ ,  $H_2/CO = 9$  and  $CO_2/CO = 3$ . The relation between methanol synthesis performance with  $H_2/CO$  and  $H_2/CO_2$  can be observed that a higher  $X_{(CO+CO_2)}$  conversion can be obtained at a high ratio of  $CO/H_2$  coupled with a low  $CO_2/H_2$  (Chein et al., 2021). Also, it can be seen that high  $X_{(CO+CO_2)}$  does not correspond to high methanol production. A high  $CO/H_2$  ratio along with a low  $CO_2/H_2$  ratio is able to meet the conditions for high methanol production along with high utility of  $H_2$ . In this work, some stoichiometric

ratios were stated for all kinetic models, and higher carbon conversion was obtained in Nestler and Graaf models as discussed above.

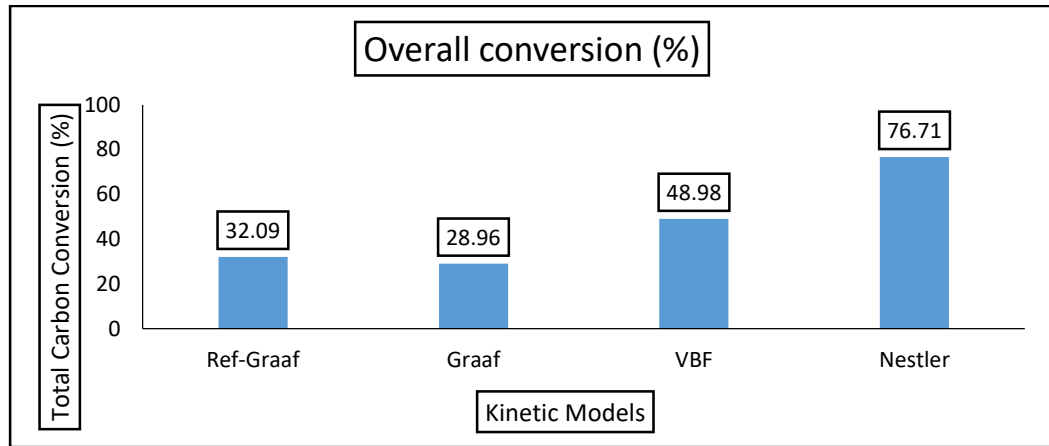


Figure 12: Overalls carbon conversion of each kinetic models

#### 4.1.3. Methanol and carbon monoxide Selectivity

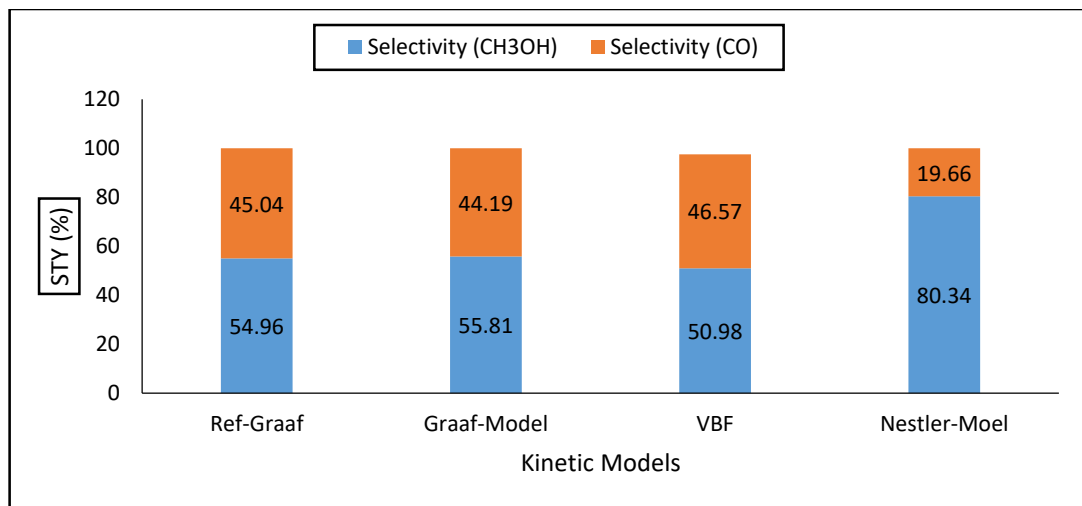


Figure 13: Methanol and carbon monoxide selectivity of each kinetic models.

Figure 13 shows the different selectivity's of methanol and carbon monoxide calculated through kinetic models simulated in the present study. The highest selectivity was obtained in Graaf and Nestler mode, 55.81 % CH<sub>3</sub>OH and 44.19 % CO, and 80.34 % CH<sub>3</sub>OH and 19.66 % CO, respectively. Slight modification in VBF at 50.91 % CH<sub>3</sub>OH and 46.56 % CO was recorded to be low in Graaf. Therefore, in Ref-Graaf and VBF, higher CO selectivity has been recorded to be low in Graaf. Thus, Ref-Graaf applied CO hydrogenation reaction or a low CO conversion to methanol or negative extent of reactions. Besides, the equilibrium of those reactions moves to the left-hand side. Tidona et al., (2013) noticed that compared to what was observed in the



RWGS reaction, the CO selectivity is higher with regard to their endothermic effect, while the other two are exothermic.

#### 4.2. Crude methanol Purification

The results in Table 9 show the different scenarios of the kinetic models studied in this work regarding methanol purification. These scenarios include parameters such as vent flow rate, recycle ratio, and the distilled flow rates of methanol and water.

Methanol purification for each model was analyzed based on the kinetic model and reactor operating conditions. The reaction results were used to set the split factor, as observed in the table, and it was found that methanol production performance is significantly affected by the recycle stream. The effect of the recycle ratio on methanol yield using syngas is evident. As the recycle ratio increases, a larger amount of unreacted syngas is returned to the methanol synthesis reactor, enhancing methanol production (Chein et al., 2021). In this case, the vent/recycle split has a significant impact on methanol synthesis.

For all design simulations of the kinetic models, except for VBF, the split factor was set at 0.02 for the Graaf, Ref-Graaf, and Nestler models, and 0.03 for the VBF model. The higher recycle ratio set in the VBF model was intended to improve methanol yield. It was observed that a low split factor negatively impacted methanol yield in the VBF model, unlike in the Graaf, Nestler, and Ref-Graaf models. The low one-pass methanol yield in the VBF model resulted in a high recycle flow, which is reflected in the higher recycle-to-feed ratio compared to the other models.

Table 9: crude methanol purification (Vent, recycle ratio, methanol and water)

Model	Vent (kmol/h)	Total recycle-Ratio	Recycled composition (kmol/h)				
			CH <sub>3</sub> OH	CO <sub>2</sub>	CO	H <sub>2</sub> O	H <sub>2</sub>
VBF	19300	15.39	1452.09	12280.21	254243.44	1159.54	353777.92
R-Graaf	4488	5.41	1450	0.00	163463.88	297.34	54686.79
Graaf	4814.06	5.78	1535.99	2045.96	162440.943	319.54	68726.58
Nestler	1383	1.67	742.33	63403.25	2709.0189	70.46	1569.23

However, a negative effect of a higher recycle ratio was observed, as mentioned by Luyben, (2010) and Nyári et al., (2022). A higher recycle flow rate causes pressure drops in various units, requiring additional recycle compressors to be installed throughout the plant. Furthermore, it was noted that a higher recycle ratio leads to an increased vent flow rate, causing more unreacted syngas to be lost.

#### 4.2.1. Distillation performance

The performance of crude methanol purification is shown in table 10, feed composition, reflux ratio, bottom product constituted with more water and top constituted with methanol and figure 13 shows the column composition profiles versus number of stages, and figure 14, column temperature profiles versus number of stages of each plant methanol design.

Then, the different plants design regarding each kinetic models, high performance is observed Ref-Graaf, where 100 % of methanol is observed in top product, and 95 % water as bottom product. In this case, it can observe that the reflux ratio in ref-Graaf is low than or comparatively of remain model, that presented less light compound to flesh such as carbon dioxide, carbon dioxide and hydrogen.

**Table 10:** performance of column distillation, include Reflux ratio, feed and output composition

Model	Reflux ratio	Feed-Composition		Bottom product		Top product		Pure CH <sub>3</sub> OH (%)
		CH <sub>3</sub> OH	H <sub>2</sub> O	CH <sub>3</sub> OH	H <sub>2</sub> O	CH <sub>3</sub> OH	H <sub>2</sub> O	
VBF	15.39	0.48	0.52	0.00	1.00	0.93	0.06	93.50
Ref-Graaf	5.41	0.62	0.37	0.20	0.80	1.00	0.00	99.99
Graaf	5.78	0.62	0.38	0.00477	0.995	0.999	0.00	99.93
Nestler	1.67	0.26	0.69	0.10	0.90	0.92	0.00	99.51

The required reflux-to-feed ratio is only about 6 % across the entire range of feed compositions for the VBF, Nestler, and Graaf kinetic models (kms), where methanol makes up 48%, 28%, and 26 % (mass), respectively, and water constitutes 52 %, 67 %, and 69 % mass, respectively. A large reflux ratio is significantly needed to remove water, which can be observed in the composition of the bottom and top products. Figure 14 shows the behavior of the vapor mole fractions along the feed stage.

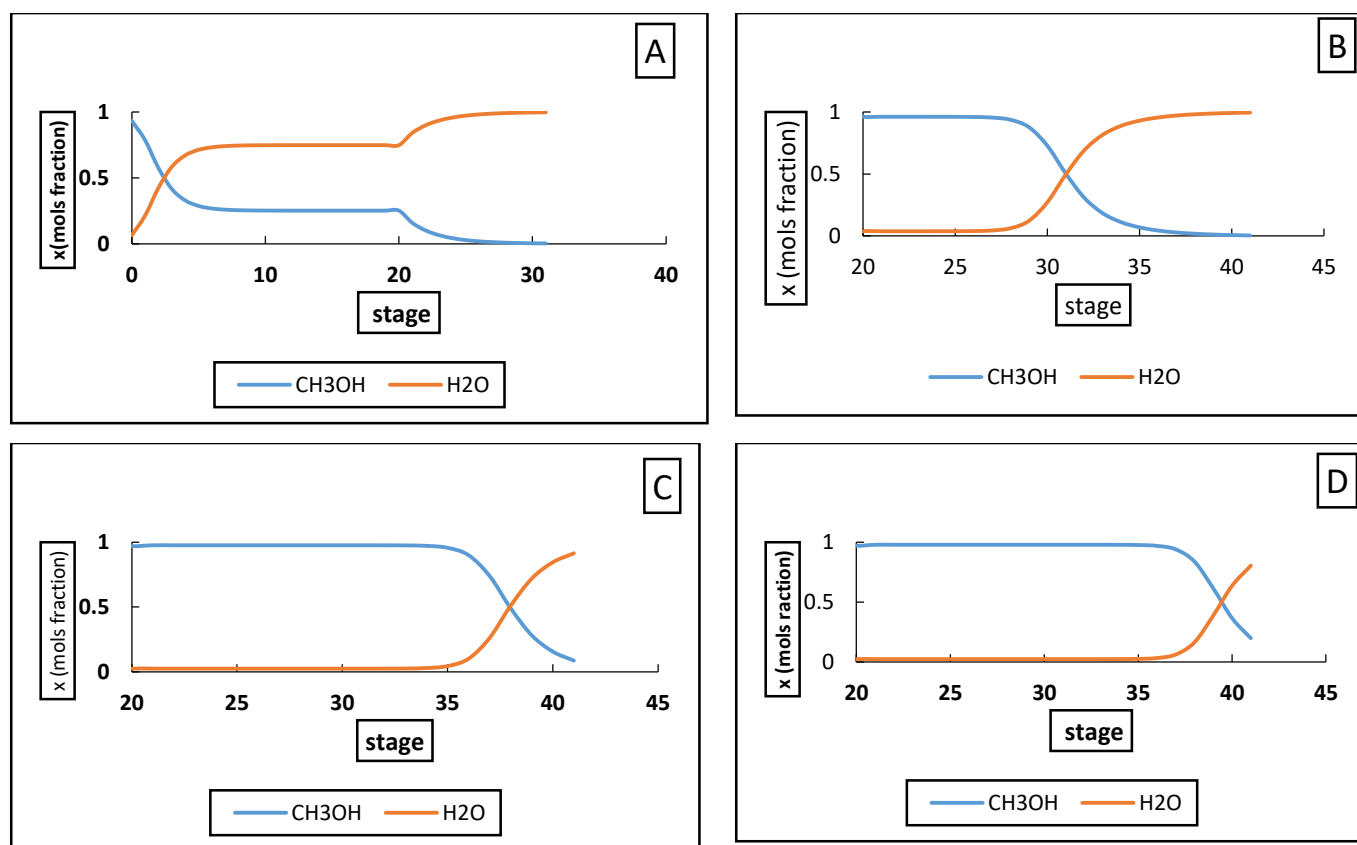


**Figure 14:** Column composition of (A)-VBF, (B)-Ref-Graaf, (C)-Graaf and (D)-Nestler KMs. In the VBF kinetic model (KM), Stage 0 is categorized as the condenser.

At this stage, the vapor composition is richer in methanol than in water. As the temperature increases, as shown in Figure 14, the methanol fraction gradually decreases once the temperature rises above 75 °C. From approximately Stage 5 to Stage 20, the temperature remains stable. During this period, the vapor becomes rich in water, and water starts to vaporize at 99.90 °C, at Stage 30, where it is observed that water is almost completely separated at a composition of 99.97 %.

In the VBF km, the temperature and vapor composition changes start around 75 °C, which is higher than in other kinetic models. This is due to the nearly equal composition of methanol and water in the feed, which causes the temperature to rise more than in other models.

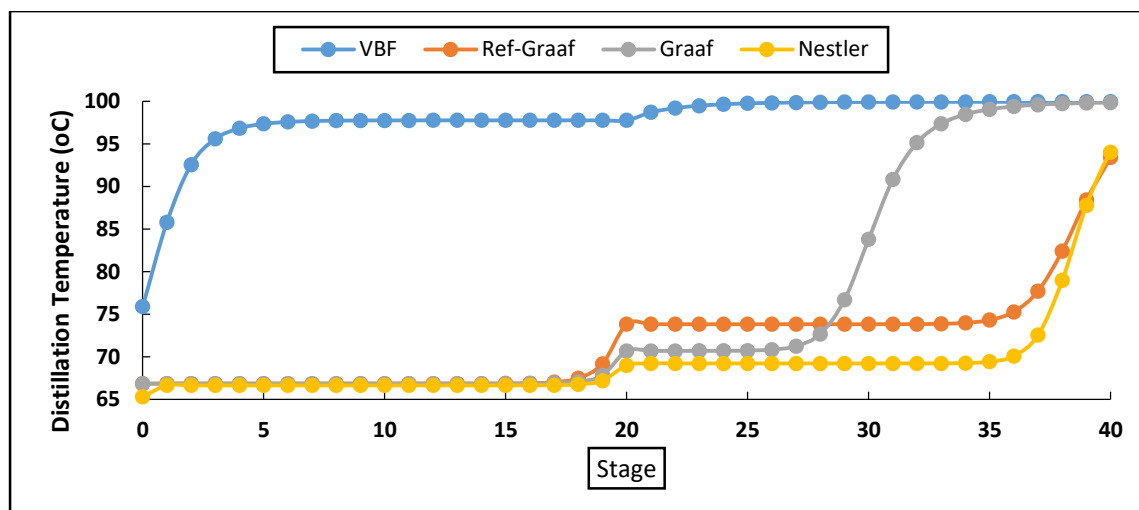


Figure 15: Column temperature profiles

In the Ref-Graaf, Graaf, and Nestler (kms), as shown in Figure 14 (B, C, and D), it is notable that methanol vapor separates from water around Stage 20. Between 67.18 °C and 73.82 °C, from Stage 18 to Stage 20, light compounds begin to evaporate. Methanol distillation occurs at 75.39 °C, where the feed composition consists of 62 % methanol and 37 % water. However, in the Nestler and Graaf models, between Stages 19 and 20, small amounts of light compounds are observed. As the process continues from Stage 20 to Stage 35 for Graaf, and up to Stage 36 for Nestler, at 70.01 °C, the vapor phase becomes richer in methanol than water, as seen in graphics C and D of Figure 13. However, the methanol purified is, 93.5 % for BVF, 99.99 % Ref-Graaf, 99.93 % Graaf, and 99.51 % for Nestler.

#### 4.3. Energy and Economic Analysis

The table 11 below shows the comparison of energy consumed and generated in the methanol synthesis models. The overall energy balance over the reactor indicates a heating duty ( $Q_h$ ) of -2.79 MW, -1.02 MW, 0.51 MW, and 19.10 MW for the VBF, Ref-Graaf, Graaf, and Nestler models, respectively. This shows that the VBF, Ref-Graaf, and Graaf models exhibit exothermic reactions, which is different from what is observed in the Nestler model.

Furthermore, the overall energy balance for each comparison of the KM processes indicates that the VBF requires more heating duty (3142.00), equivalent to 11,794.5 Mt/yr of steam, a cooling duty of 1146.0 MW that can be supplied in the form of 2136.38 t/yr of cooling water (CW), and 211.03 MW of electricity. In contrast, the other kms show different scenarios, as observed in the table below. The Ref-Graaf km presents lower heating duty, cooling duty, cooling water, and steam requirements compared to the Graaf and Nestler models.

Table 11: Energy and Utility Consumption Comparison across Methanol Synthesis Models

Parameter	Unit	Model			
		VBF	Ref-Graaf	Graaf	Nestler
Heat duty of reactor	MW	-2.79	-1.02	-0.51	19.10
Reboil heat duty	MW	433.32	345.80	652.90	789.20
Condensor heat duty	MW	352.70	236.70	532.90	658.40
Cooling utilities	MW	1146.00	1780.00	806.30	1739.00
Heating Utilities	MW	3142.00	678.90	1915.00	1126.00
Overall Utilities Duty	MW	4288.00	2458.90	2721.30	2865.00
Cooling utilities cost	M/yr	99.32	64.63	78.94	70.03
Heating Utilities cost	MUS\$/yr	77.30	42.06	39.89	79.28
Total Utilities cost	M/yr	176.62	106.69	118.83	149.31
CO <sub>2</sub> emission	t/yr	862.70	460.00	625.40	576.50
Cooling water	MMt/yr	2136.38	1115.87	1309.29	1173.36
Electricity Used	MW	211.03	173.47	215.53	218.02
Steam	Mt/yr	11794.50	10176.80	16998.92	15822.06

The behavior of the VBF km was discussed and observed in the study by Nyári et al., (2022), which compared three KMs: VBF, Kiss, and Slotboom. The VBF presented high heating and cooling duties. In a study conducted by Abdelaziz et al., (2017) the VBF km exhibited a heating duty of 52.8 MW, which is equivalent to 689,000 t/yr of steam, along with high electricity consumption. Additionally, research by Luyben, (2010) reported a heating duty of 102 MW. However, the high cooling and heating duties it can be affects significantly in the cost, as shows in figure 16 below.

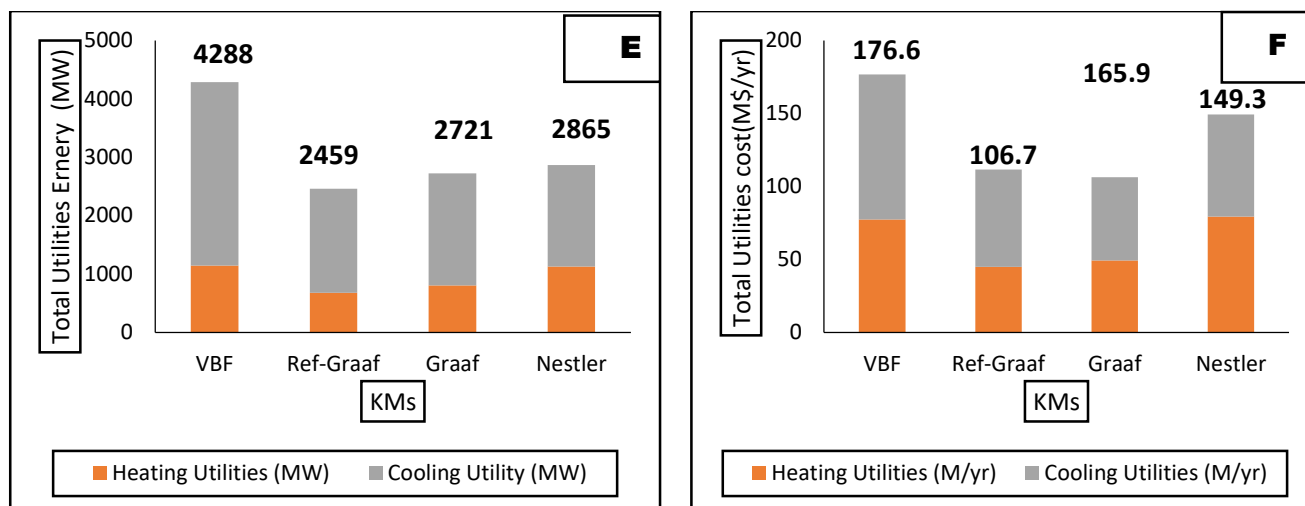


**Figure 16:** The Heating and cooling Utilities energy and cost (E and F).

However, the Ref-Graaf km presented the lowest utilities cost, as can be observed in Table 15, particularly in terms of required electricity and cooling water (CW). On the other hand, the heating duty required for the reboiler and condenser in the Ref-Graaf model is also lower, with a reduced heating duty for condensing methanol and recovering steam in the reboiler. In comparison, other KM scenarios, such as the VBF, show higher utilities costs and significantly higher heating duties in both the reboiler and condenser.

#### 4.3.1. Heat integration design

Therefore, the objective is to design an integrated energy network for the selected kms for methanol production (water cooling), applying the established Pinch Analysis principles in designing an alternative energy-efficient HEN by using Aspen Energy Analysis commercial software. Energy streams data are extracted from the developed processes design. The extracted data consist of temperature, heat duty, and heat capacity of each process stream. The utility data and the cost data are found to be helpful in determining the energy cost and capital investment. However, the data of the selected processes was extracted in calculated and are given in figure 17, represented as total utilities integrated (G) and total integrated utilities cost (H). Heat integration studies are performed for the process flow shown in Figure 4 of the methodology chapter. At the beginning of the analysis, data are extracted from the steady state, and the grid diagram is constructed for each km's process simulation. The composite curves represent the heating and cooling demand of the process corresponding to the temperature range. However, the curves establish the energy targets prior to the design, and the maximum quantity of energy recovery can thereby be calculated. The red curves represent the hot steam, and the blue curves represent the cooled steam.

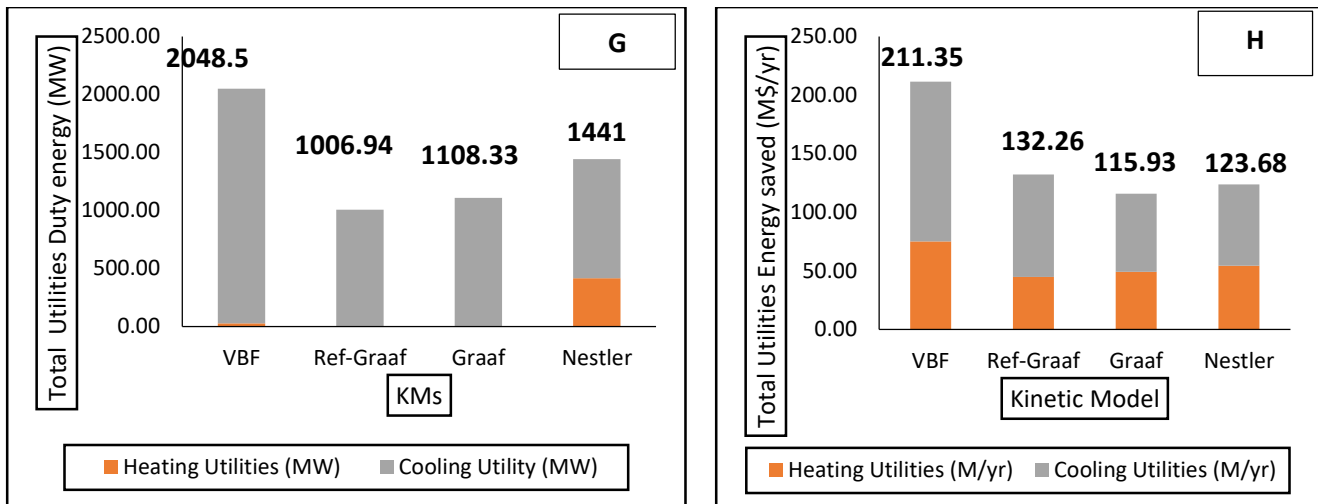


Figure 17: Total steam utilities (HEN) integrated (G) and the integrated utilities cost saved (H)

The closed gap in the diagram indicates the  $\Delta T_{min}$ , which is the minimum driving force for heat exchange. The pinch point is where the two curves come closest together, and the temperature difference between the two composite curves is  $\Delta T_{min}$ . Economic efficiency is determined by  $\Delta T_{min}$ , as it affects the heat exchange area. For all km's process simulations,  $\Delta T_{min}$  is identified as 10 °C, as shown in Figure 18.

Before energy integration, it was previously discussed that the VBF km had the highest energy duty, while the Ref-Graaf km had a lower energy duty compared to Graaf and Nestler. However, for the VBF km, the cold utility heat was around 2051.37 MW, and after integration, approximately 663.95 MW of heat was recovered, resulting in a 52.23 % energy saving or reduction. It can also be observed that steam costs were saved to 211.35 M\$/yr.

For the Ref-Graaf km, which initially had a low total utility duty of 2459 MW before heat integration, the heating duty was reduced to zero MW after integration, and the cooling duty decreased to 2022.53 MW, corresponding to a 59.05% energy saving, with a recovered heat duty of 357.13 MW, and the steam cost saved 132.26 M\$/yr.

In the case of the Graaf KM, the cold utility heat was 1110.73 MW, with a recoverable heat of 381.02 MW, resulting in 59.27 % energy saved. The heating utilities were reduced to zero MW after integration, and the cooling utility decreased to 1108.33 MW, the cost of steam was also saved 115.93 M\$/yr.

Finally, for the Nestler km, the energy duty of the heating utility was initially 1126 MW, which was reduced to 414.40 MW after heat integration, while the cooling utility decreased from 1739 MW to 1026.63 MW. The recovered heat was about 609.09 MW, and the total energy saved was 49.02 %.

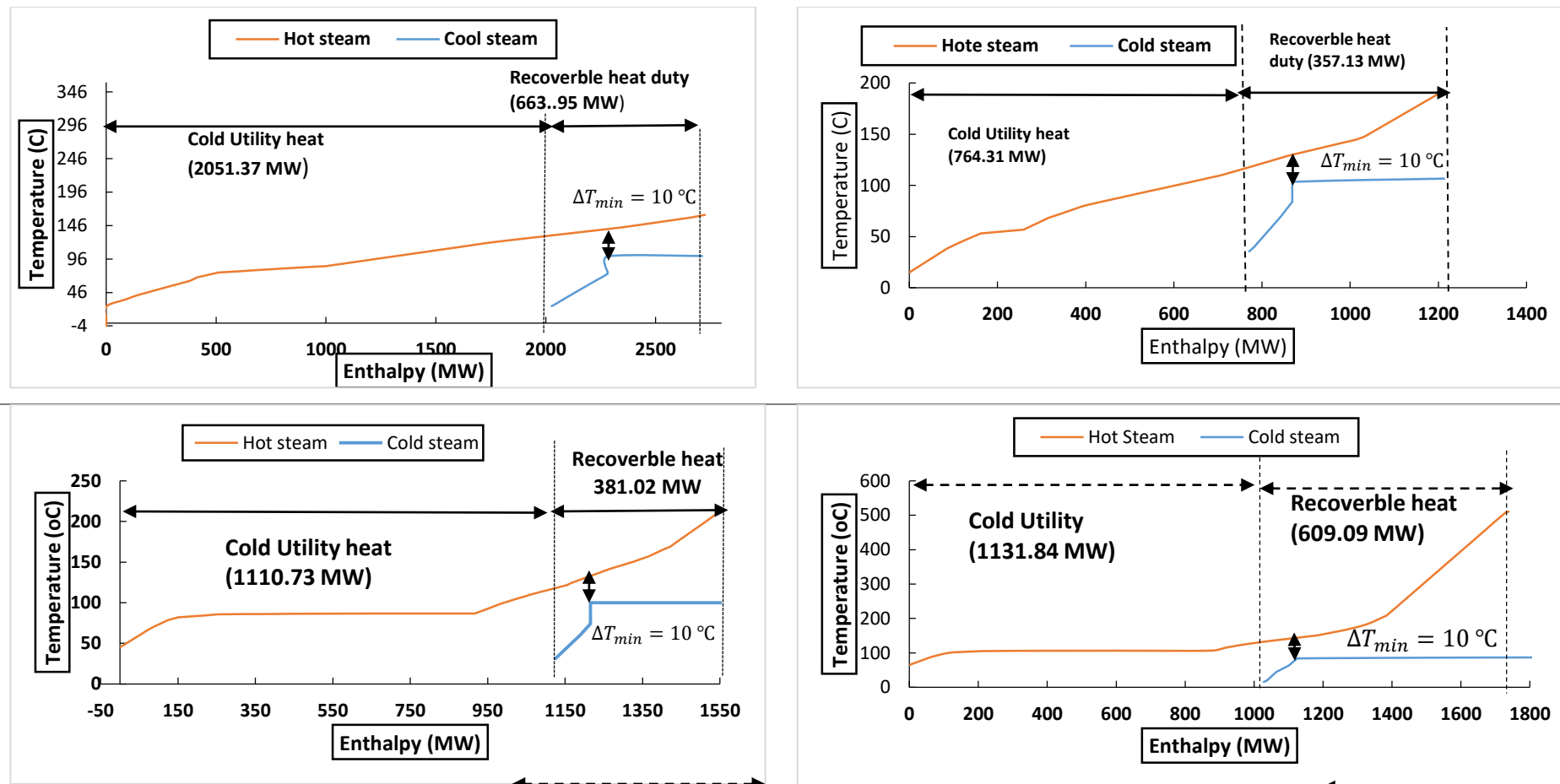


**Figure 18:** Energy performance of steam cooling VBF (I), Ref-Graaf (J), Graaf (K) and Nestler (L).



### 4.3.2. Economic Analysis

The levelized cost of methanol is calculated according to equation 11, by taking into account the CAPEX, the OPEX, the methanol mass flow rate, and the levelized lifetime of the process. All the results are summarized in (figure 19, 20), levelized cost of MeOH including hydrogen cost and levelized cost of MeOH without cost hydrogen in M\$/tonnes of methanol produced per year.

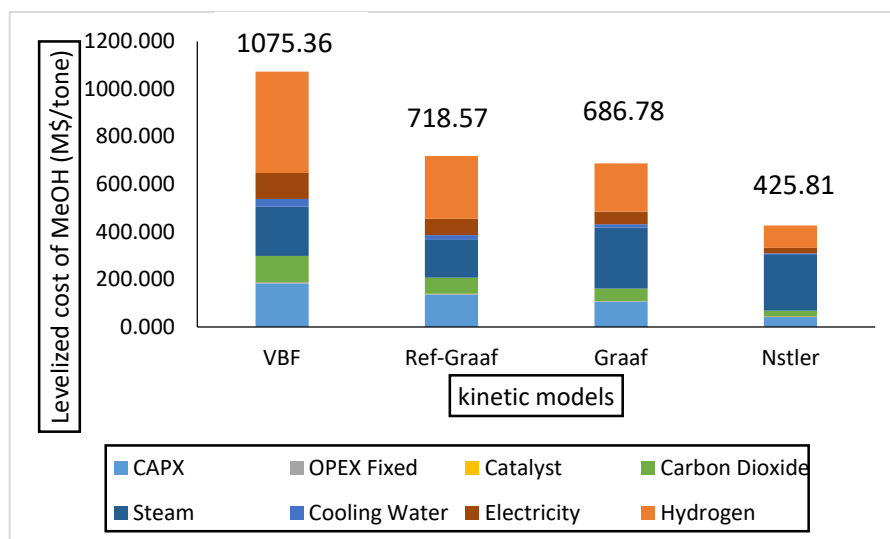


Figure 19: levelized cost of MeOH including cost of hydrogen in M\$ per tonnes of methanol.

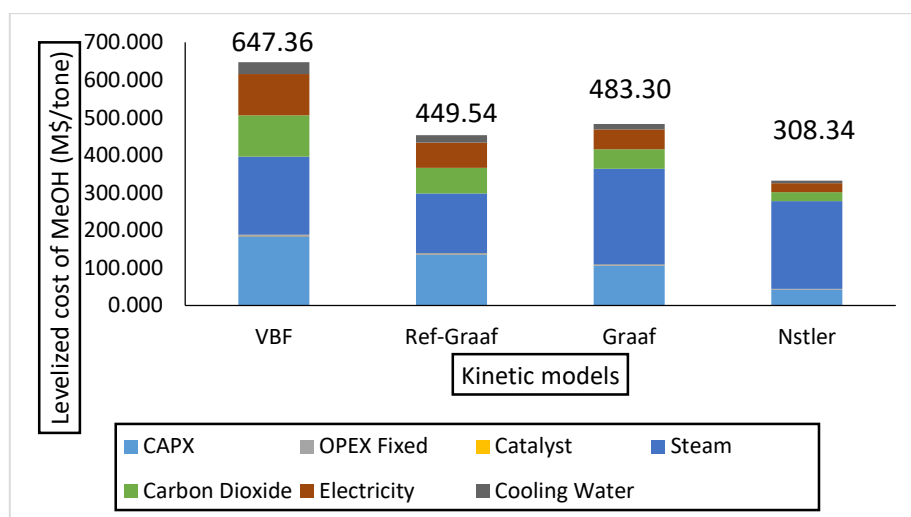


Figure 20: levelized cost of MeOH without hydrogen cost in M\$ per tonnes of methanol.

The production cost of methanol equal to 1075.36 M\$/ton to VBF, 718.5 M\$/ton to Ref-Graaf, 686.78 M\$/ton to Graaf and 425.81 M\$/ton to Nesleer. While the production cost of methanol without including hydrogen, is equal to 641.93 M\$/ton to VBF, 449.61 M\$/ton to Ref-Graaf,

480.14 M\$/ton to Graaf and 329.85 M\$/ton to Nestler. In particular, the results of levelized cost shows that the pure hydrogen stream has high influence in production cost of methanol, what can see in figure (21 and 22), the percentage of OPEX, with and without hydrogen including.

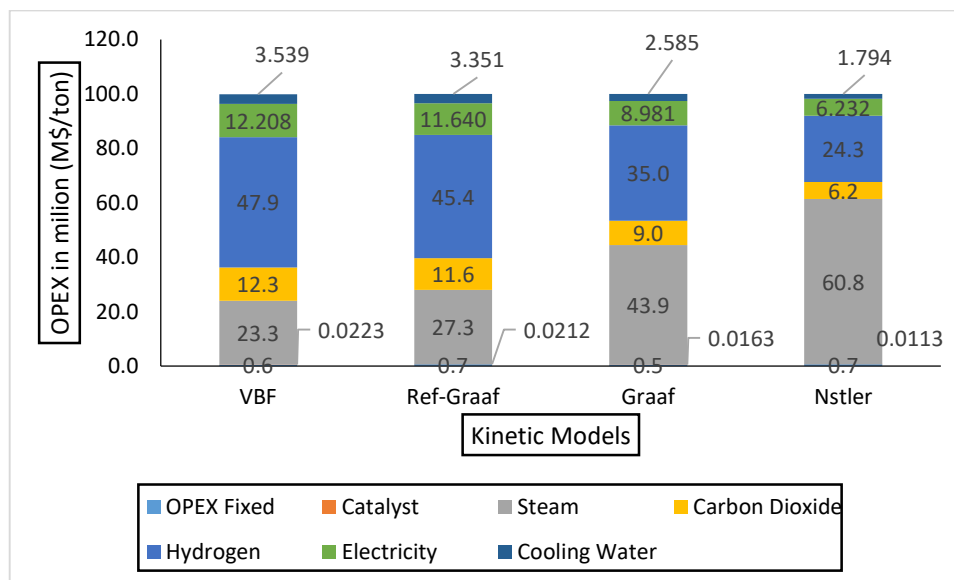


Figure 21: Comparison of annual operational expense of the developed methanol plant using kinetic models study, total OPEX.

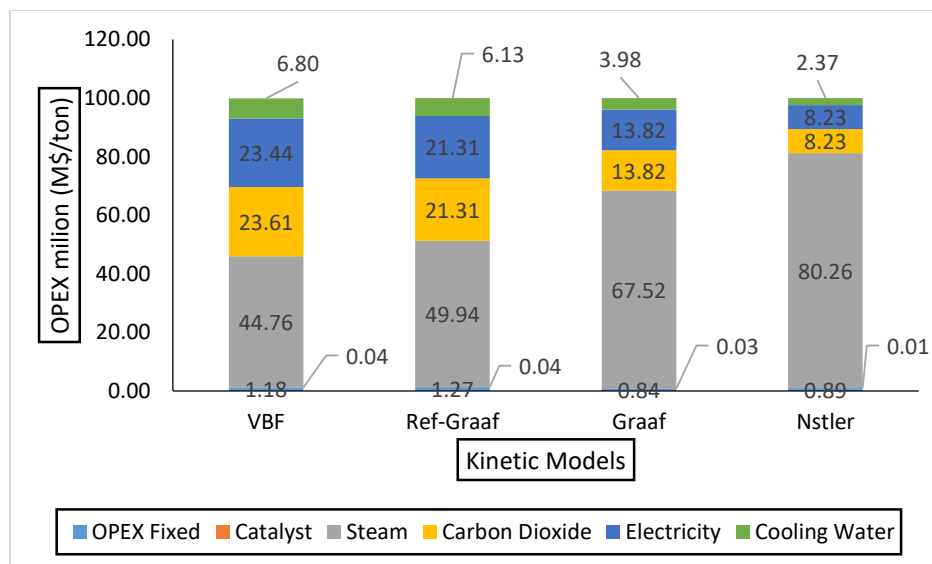


Figure 22: Comparison annual OPEX of the developed methanol plant using kinetic models without hydrogen cost.

Therefore, the comparison of annual OPEX of the developed methanol plant using different kinetic models, with and without hydrogen cost, it is seen that hydrogen cost, affect

significantly in OPEX, to VBF and Ref-Graaf, where, 47.90 % reduced to 23.61 % to VBF, and 45.60 % reduced to 21.31 % to Ref-Graaf, while the Graaf and Nestler, were the KMs that presented low OPEX, 35.00 % reduced to 13.82 % to Graaf, and 24.33 % reduced to 8.23 %. How, the explaining of the higher cost is related of the less methanol produced, also in the quantity of CO<sub>2</sub> recycled. And the other parameter is also considered to evaluate the OPEX, such as steam, cooling water, catalyst, fixed OPEX, in this high stem (80.26 %) to Nestler is observed. Moreover, the catalyst, and fixed OPEX has less influence in the variation cost in the total OPEX, kindly at Graaf and Nestler km's where observed, 0.03 % and 0.01 % respectively. In the study conducted by Abdelaziz et al., (2017), where observed low methanol production cost of VBF model when impregnated, series of column to water remove, meaning that cooling water and steam can affect in methanol investment cost. While, J. Portha et al., (2021), reported that the OPEX related to the consumption of low pressure steam. Concerning the large quantity of cooling water, this consumption can be explained by the cooling requirement. The considerably larger mass flow of the recycle steam also manifests in the higher share of electricity cost (Nyári et al., 2022). However, the significantly larger share of electricity cost with the VBF model is due the higher mass rate in the recycle steam. Meanwhile, the Ref-Graaf, and Nestler have low electricity cost and low mass flow rate in the recycle steam. The annual methanol produced can affect the rate of fixed OPEX, but the km's design plant have same the fixed OPEX, as that is independent of the consumption and production values.

## CHAPATER 5 – CONCLUSION, RECOMMENDATION AND LIMITATION

This chapter presented the close section of this research, include conclusion and recommendation, and also the limitation was being faced during the study.

### 5.1. Conclusion

The investigation was focused in comparative analysis of methanol production via CO<sub>2</sub> hydrogenation using different kinetic models. However, after deep investigation was conclude that, the comparative analysis of methanol production via CO<sub>2</sub> hydrogenation using different kinetic models, is bring a benefit and environmental sustainability in the carbon emission.

Therefore, the was selected VBF, Ref-Graaf, Graaf and Nestler kms, the temperature, pressure, reactor tube diameter, length, and thermodynamic proprieties package was used as initial condition to validation the kms using aspen Hysys. The models were studied was simulated in steady state, and using one-pass sensitivity analysis of pressure and temperature, which provided that there is a significant difference in how the models predict methanol yield and CO<sub>2</sub> conversation. However, it was shown that the temperature has its significant effect in methanol yield, the VBF kms presented endothermic effect, comparatively with Ref-Graaf, Graaf, and high exothermic effect observed in Nestler kms, and high yield observed on the Nestler. And the conversion and methanol selectivity: Nestler has obtained overall conversion (76.71 %), and methanol STY (80.33 %); for Ref-Graaf with 32.09 % of overall conversion and 54.96 % of methanol STY; Graaf 28.96 % of overall conversion and 54.96 % % STY; and VBF has obtained 48.97 % overall conversion and 50.96 % of STY.

Then, design heat integration performed using Aspen energy analysis of the four kms, was observed that the VBF, has high utilities energy 4288, and 52.23 % was saved after HI; Ref-Graaf and Graaf have high saved energy and cost 59.04 % and 59.07 %; and Nestler 49.02 % of energy saved. However, the pinch analysis shows that, the Nestler is the kms has high revocable heat, 609.09 MW, while the VBF was of the km that presented high cold utility heat, 2051.37 MW.

Moreover, the TEA studies, and the four kms were implemented in its methanol plant design to study their effect. The application of different KMs results in different utility usages. So the newest, Ref-Graaf and Nestler models are compared with older VBF and Graaf models. The Ref-Graaf model has high LCM<sub>MeOH</sub>, 718.57 M\$/yr, comparatively with Original Graaf model, 686.78 M\$/yr, include hydrogen stream cost, without hydrogen steam cost, Ref-Graaf is low LCM<sub>MeOH</sub>, 449.54 M\$ than Graaf LCM<sub>MeOH</sub>, 483.30 M\$/yr. However, its notable that, Nestler

has presented the low LCM<sub>OH</sub>, 425.81 M\$/yr, include hydrogen cost, and 308.34 M\$/yr without hydrogen cost.

Finally, the Ref-Graaf and Nestler are the newest kms that can in the future potentially and environmental sustainability in the methanol production because showed, high methanol yield, methanol selectivity, and economically viable. However, this conclusion it not definitively meanwhile some future improvement should be done, the reason why we left the recommendation and the limitation found in this study.

## 5.2. Recommendation

1. The kms design simulation was done in steady state, and we recommend the future investigation of Ref-Graaf and Nestler to be simulated in dynamic state, and also optimization the process simulation in steady and dynamic states.
2. The Ref-Graaf and Nestler are the kms that presented high methanol yield, and low LCM<sub>OH</sub> and low OPEX, we recommend to perform the sensitivity analysis doing preferably lab experiments on the given catalyst and raw materials should be conducted an a kms should be fitted to the data.
3. Because the limitation of Aspen Hysys we recommend to simulation those newest km's (Ref-Graaf and Nestler) using other simulation software program, such as COCO, DWSIM, Aspen Plus, etc.

## 5.3. Limitation

Due the simulation of KMs design methanol plant, we face many difficult what concern of KM and Aspen Hysys, at which can give not precise and accuracy results:

First, aspen Hysys is in LHHW models and the kinetic rate equation depends on the volume of reactor, not of catalyst mass, and some the kms, such as Ref-Graaf, Graaf and Nestler do not correspond of Aspen Hysys proprieties, require high domain in math to drive the rate equation into LHHW and in volume of catalyst, and this reason took to exclude the some kms with complex rate equation. And the Aspen Hysys is slightly limited in thermodynamic proprieties.

## BIBLIOGRAPHY

- Aasberg-Petersen, K., Stub Nielsen, C., & Dybkjr, I. (2007). Very Large Scale Synthesis Gas Production and Conversion to Methanol or Multiple Products. *Studies in Surface Science and Catalysis*, 167, 243–248. [https://doi.org/10.1016/S0167-2991\(07\)80139-X](https://doi.org/10.1016/S0167-2991(07)80139-X)
- Abdelaziz, O. Y., Hosny, W. M., Gadalla, M. A., Ashour, F. H., Ashour, I. A., & Hulteberg, C. P. (2017). Novel process technologies for conversion of carbon dioxide from industrial flue gas streams into methanol. *Journal of CO<sub>2</sub> Utilization*, 21(June), 52–63. <https://doi.org/10.1016/j.jcou.2017.06.018>
- Akinosho, T. (2023). *Maximum gas price of \$ 6.5/MMBtu “Not excessive”, Sasol tells south africa regulator.* Africa + Oil Gas Report. <https://africaoilgasreport.com/2023/07/gas-monetization/maximum-gas-price-of-6-5-per-thousand-cubic-feet-not-excessive-sasol-tells-south-african-regulator/>
- AspenTech. (2005). *Hysys Operations Guide-aspenTech driving process profitability.*
- Balopi, B., Agachi, P., & Danha. (2019). Methanol synthesis chemistry and process engineering aspects - A review with consequence to Botswana chemical industries. *Procedia Manufacturing*, 35, 367–376. <https://doi.org/10.1016/j.promfg.2019.05.054>
- Bermúdez, J. M., Ferrera-Lorenzo, N., Luque, S., Arenillas, A., & Menéndez, J. A. (2013). New process for producing methanol from coke oven gas by means of CO<sub>2</sub> reforming. Comparison with conventional process. *Fuel Processing Technology*, 115, 215–221. <https://doi.org/10.1016/j.fuproc.2013.06.006>
- Bisotti, F., Fedeli, M., Prifti, K., Galeazzi, A., Dell’Angelo, A., Barbieri, M., Pirola, C., Bozzano, G., & Manenti, F. (2021). Century of Technology Trends in Methanol Synthesis: Any Need for Kinetics Refitting? *Industrial and Engineering Chemistry Research*, 60(44), 16032–16053. <https://doi.org/10.1021/acs.iecr.1c02877>
- Bisotti, F., Fedeli, M., Prifti, K., Galeazzi, A., Dell’Angelo, A., & Manenti, F. (2022). Impact of Kinetic Models on Methanol Synthesis Reactor Predictions: In Silico Assessment and Comparison with Industrial Data. *Industrial and Engineering Chemistry Research*, 61(5), 2206–2226. <https://doi.org/10.1021/acs.iecr.1c04476>
- Chein, R. Y., Chen, W. H., Chyuan Ong, H., Loke Show, P., & Singh, Y. (2021). Analysis of methanol synthesis using CO<sub>2</sub> hydrogenation and syngas produced from biogas-based reforming processes. *Chemical Engineering Journal*, 426(June), 130835.

<https://doi.org/10.1016/j.cej.2021.130835>

- Cui, X., & Kær, S. K. (2019). Thermodynamic analyses of a moderate-temperature process of carbon dioxide hydrogenation to methanol via reverse water-gas shift with in situ water removal [Research-article]. *Industrial and Engineering Chemistry Research*, 58(24), 10559–10569. <https://doi.org/10.1021/acs.iecr.9b01312>
- Dalena, F., Senatore, A., Marino, A., Gordano, A., Basile, M., & Basile, A. (2018a). Methanol Production and Applications: An Overview. In *Methanol: Science and Engineering* (pp. 3–28). Elsevier B.V. <https://doi.org/10.1016/B978-0-444-63903-5.00001-7>
- Dalena, F., Senatore, A., Marino, A., Gordano, A., Basile, M., & Basile, A. (2018b). Methanol Production and Applications: An Overview. *Methanol: Science and Engineering*, 3–28. <https://doi.org/10.1016/B978-0-444-63903-5.00001-7>
- Gabrielli, P., Gazzani, M., & Mazzotti, M. (2020). The Role of Carbon Capture and Utilization, Carbon Capture and Storage, and Biomass to Enable a Net-Zero-CO<sub>2</sub> Emissions Chemical Industry. *Industrial and Engineering Chemistry Research*, 59(15), 7033–7045. <https://doi.org/10.1021/acs.iecr.9b06579>
- Gao, N., Li, A., Quan, C., Qu, Y., & Mao, L. (2012). Characteristics of hydrogen-rich gas production of biomass gasification with porous ceramic reforming. *International Journal of Hydrogen Energy*, 37(12), 9610–9618. <https://doi.org/10.1016/j.ijhydene.2012.03.069>
- Gao, P., Zhang, L., Li, S., Zhou, Z., & Sun, Y. (2020). Novel heterogeneous catalysts for CO<sub>2</sub> hydrogenation to liquid fuels. *ACS Central Science*, 6(10), 1657–1670. <https://doi.org/10.1021/acscentsci.0c00976>
- Graaf, G. H., Stamhuis, E. J., & Beenackers, A. A. C. M. (1988). Kinetics of low-pressure methanol synthesis. *Chemical Engineering Science*, 43(12), 3185–3195. [https://doi.org/10.1016/0009-2509\(88\)85127-3](https://doi.org/10.1016/0009-2509(88)85127-3)
- Henkel, T. A. (2011). *Modellierung von Reaktion und Stofftransport in geformten Katalysatoren am Beispiel der Methanolsynthese*. 210.
- Huš, M., Dasireddy, V. D. B. C., Strah Štefančič, N., & Likozar, B. (2017). Mechanism, kinetics and thermodynamics of carbon dioxide hydrogenation to methanol on Cu/ZnAl<sub>2</sub>O<sub>4</sub> spinel-type heterogeneous catalysts. *Applied Catalysis B: Environmental*, 207, 267–278. <https://doi.org/10.1016/j.apcatb.2017.01.077>
- Kim, I., Lee, G., Jeong, H., Park, J. H., & Jung, J. C. (2017). Bifunctionality of Cu/ZnO

- catalysts for alcohol-assisted low-temperature methanol synthesis from syngas: Effect of copper content. *Journal of Energy Chemistry*, 26(3), 373–379. <https://doi.org/10.1016/j.jechem.2017.02.003>
- Lange, J. (2001). *Methanol synthesis : a short review of technology improvements*. 64, 3–8.
  - Li, D., Xu, F., Tang, X., Dai, S., Pu, T., Liu, X., Pengfei Tian, F. X., Xu, Z., & Zhu, I. E. W. & M. (2022). Induced activation of the commercial Cu/ZnO/Al<sub>2</sub>O<sub>3</sub> catalyst for the steam reforming of methanol. *Nature Catalyst*, 5, 99–108. <https://doi.org/https://doi.org/10.1038/s41929-021-00729-4>
  - Lim, H., Park, M., Kang, S., Chae, H., Bae, J. W., & Jun, K. (2009). *Modeling of the Kinetics for Methanol Synthesis using Cu / ZnO / Al<sub>2</sub>O<sub>3</sub> / ZrO<sub>2</sub> Catalyst : Influence of Carbon Dioxide during Hydrogenation*. 10448–10455.
  - Luyben, W. L. (2010). Design and control of a methanol reactor/column process. *Industrial and Engineering Chemistry Research*, 49(13), 6150–6163. <https://doi.org/10.1021/ie100323d>
  - Marcos, F. C. F., Cavalcanti, F. M., Petrolini, D. D., Lin, L., Betancourt, L. E., Senanayake, S. D., Rodriguez, J. A., Assaf, J. M., Giudici, R., & Assaf, E. M. (2022). Effect of operating parameters on H<sub>2</sub>/CO<sub>2</sub> conversion to methanol over Cu-Zn oxide supported on ZrO<sub>2</sub> polymorph catalysts: Characterization and kinetics. *Chemical Engineering Journal*, 427(May 2021). <https://doi.org/10.1016/j.cej.2021.130947>
  - Meyer, J. J., Tan, P., Apfelbacher, A., Daschner, R., & Hornung, A. (2016). *Modeling of a Methanol Synthesis Reactor for Storage of Renewable Energy and Conversion of CO<sub>2</sub> – Comparison of Two Kinetic Models*. 2, 233–245. <https://doi.org/10.1002/ceat.201500084>
  - Moulijn, J., Makkee, M., & Diepen, A. (2013). Chemical Process Technology. In Wiley (Ed.), *Chemical process technology* (Second Edi).
  - Navarrete, A., & Zhou, Y. (2024). *THE PRICE OF GREEN HYDROGEN: HOW AND WHY WE ESTIMATE FUTURE PRODUCTION COSTS*. Internacional Council of Clean Transportation (ICCT). <https://theicct.org/the-price-of-green-hydrogen-estimate-future-production-costs-may24/>
  - Nestler, F., Schütze, A. R., Ouda, M., Hadrich, M. J., Schaadt, A., Bajohr, S., & Kolb, T. (2020). Kinetic modelling of methanol synthesis over commercial catalysts: A critical assessment. *Chemical Engineering Journal*, 394(December 2019), 124881.



<https://doi.org/10.1016/j.cej.2020.124881>

- Nguyen, T. B. H., & Zondervan, E. (2019). Methanol production from captured CO<sub>2</sub> using hydrogenation and reforming technologies- environmental and economic evaluation. *Journal of CO<sub>2</sub> Utilization*, 34(May), 1–11. <https://doi.org/10.1016/j.jcou.2019.05.033>
- Nyári, J., Izbassarov, D., Toldy, Á. I., Vuorinen, V., & Santasalo-Aarnio, A. (2022). Choice of the kinetic model significantly affects the outcome of techno-economic assessments of CO<sub>2</sub>-based methanol synthesis. *Energy Conversion and Management*, 271(June). <https://doi.org/10.1016/j.enconman.2022.116200>
- NYSERDA. (2004). *Hydrogen fact sheet Hydrogen Production – Steam Methane Reforming (SMR)*. [www.nyserda.org](http://www.nyserda.org)
- Olajire, A. A. (2013). Valorization of greenhouse carbon dioxide emissions into value-added products by catalytic processes. *Journal of CO<sub>2</sub> Utilization*, 3–4, 74–92. <https://doi.org/10.1016/j.jcou.2013.10.004>
- Osman, A. I., Mehta, N., Elgarahy, A. M., Hefny, M., Al-Hinai, A., Al-Muhtaseb, A. H., & Rooney, D. W. (2022). Hydrogen production, storage, utilisation and environmental impacts: a review. In *Environmental Chemistry Letters* (Vol. 20, Issue 1). <https://doi.org/10.1007/s10311-021-01322-8>
- Ott, J., Gronemann, V., Florian, P., Eckhard, F., Grossmann, G., Burkhard, K. D., Weiss, G., & Write, C. (2012). Methanol. *Encyclopedia of Industrial Chemistry*.
- Palma, V., Meloni, E., Ruocco, C., Martino, M., & Ricca, A. (2018). State of the Art of Conventional Reactors for Methanol Production. *Methanol: Science and Engineering*, 29–51. <https://doi.org/10.1016/B978-0-444-63903-5.00002-9>
- Portha, J. F., Uribe-Soto, W., Commenge, J. M., Valentin, S., & Falk, L. (2021). Techno-economic and carbon footprint analyses of a coke oven gas reuse process for methanol production. *Processes*, 9(6), 1–24. <https://doi.org/10.3390/pr9061042>
- Portha, J., Uribe-soto, W., Commenge, J., & Falk, L. (2021). *Techno-Economic and Carbon Footprint Analyses of a Coke Oven Gas Reuse Process for Methanol Production*. 1–24.
- Poto, S., Vico, D., Berkel, V., Gallucci, F., & Neira, M. F. (2022). Kinetic modelling of the methanol synthesis from CO<sub>2</sub> and H<sub>2</sub> over a CuO / CeO<sub>2</sub> / ZrO<sub>2</sub> catalyst : The role of CO<sub>2</sub> and CO hydrogenation. *Chemical Engineering Journal*, 435(P2), 134946. <https://doi.org/10.1016/j.cej.2022.134946>

- Ramon L. Espino, & Pletzke, T. S. (1975). *Methanol Production*.
- Shahbaz, M., yusup, S., Inayat, A., Patrick, D. O., & Ammar, M. (2017). The influence of catalysts in biomass steam gasification and catalytic potential of coal bottom ash in biomass steam gasification: A review. *Renewable and Sustainable Energy Reviews*, 73(November 2015), 468–476. <https://doi.org/10.1016/j.rser.2017.01.153>
- Struis, R. P. W. J., Stucki, S., & Wiedorn, M. (1996). A membrane reactor for methanol synthesis. *Journal of Membrane Science*, 113(1), 93–100. [https://doi.org/10.1016/0376-7388\(95\)00222-7](https://doi.org/10.1016/0376-7388(95)00222-7)
- Tidona, B., Koppold, C., Bansode, A., Urakawa, A., & Rudolf Von Rohr, P. (2013). CO<sub>2</sub> hydrogenation to methanol at pressures up to 950 bar. *Journal of Supercritical Fluids*, 78, 70–77. <https://doi.org/10.1016/j.supflu.2013.03.027>
- Trop, P., Anicic, B., & Goricanec, D. (2014). Production of methanol from a mixture of torrefied biomass and coal. *Energy*, 77, 125–132. <https://doi.org/10.1016/j.energy.2014.05.045>
- Vanden Bussche, K. M., & Froment, G. F. (1996). A steady-state kinetic model for methanol synthesis and the water gas shift reaction on a commercial Cu/ZnO/Al<sub>2</sub>O<sub>3</sub> catalyst. *Journal of Catalysis*, 161(1), 1–10. <https://doi.org/10.1006/jcat.1996.0156>
- Wiesberg, I. L., Luiz, J., Medeiros, D., Alves, R. M. B., Coutinho, P. L. A., & Araújo, O. Q. F. (2016). Carbon dioxide management by chemical conversion to methanol : HYDROGENATION and BI-REFORMING. *ENERGY CONVERSION AND MANAGEMENT*. <https://doi.org/10.1016/j.enconman.2016.04.041>
- Zangeneh, F. T., Sahebdehfar, S., & Ravanchi, M. T. (2011). Conversion of carbon dioxide to valuable petrochemicals: An approach to clean development mechanism. *Journal of Natural Gas Chemistry*, 20(3), 219–231. [https://doi.org/10.1016/S1003-9953\(10\)60191-0](https://doi.org/10.1016/S1003-9953(10)60191-0)

## APPENDIX 1: GRAPHICS

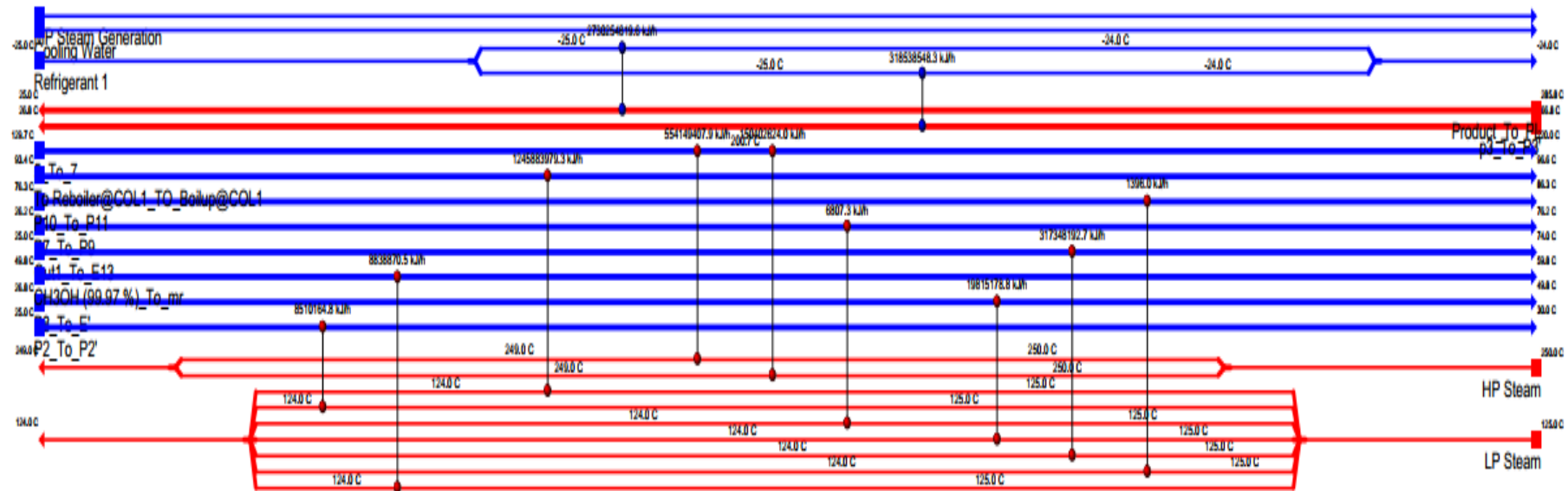


Figure A 1: Profile of HEN-integration of Ref-Graaf kinetic model

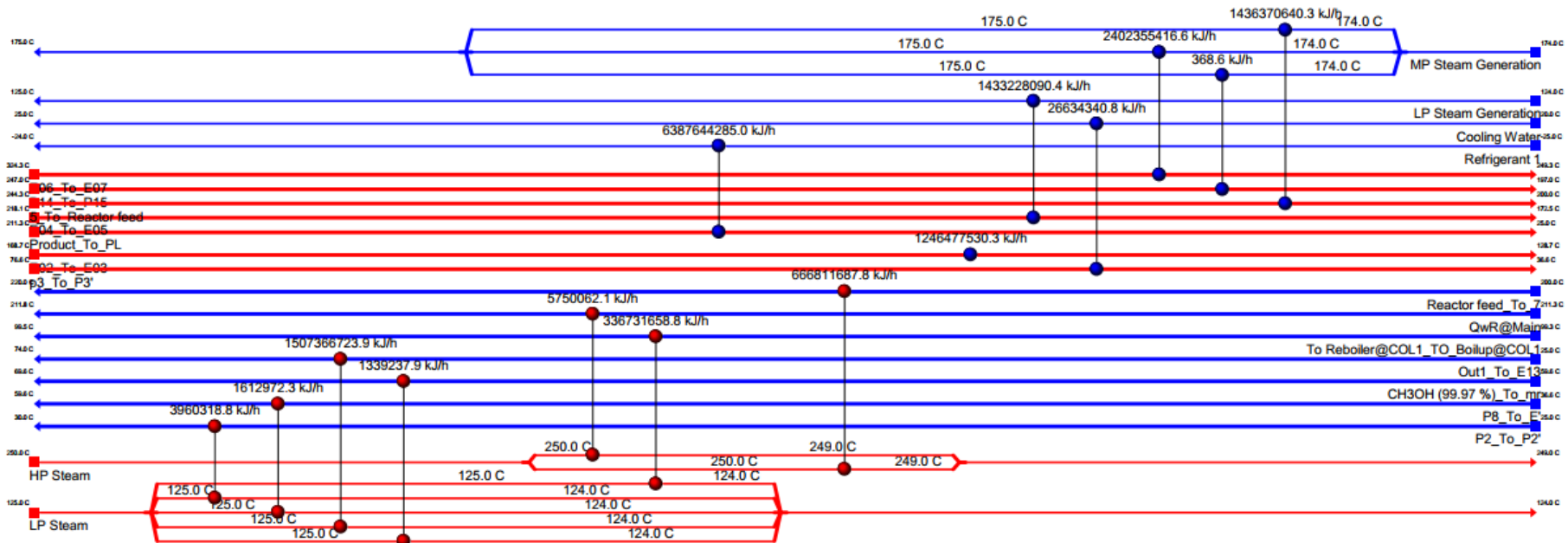


Figure A 2: profile of HEN-integration of VBF kinetic models

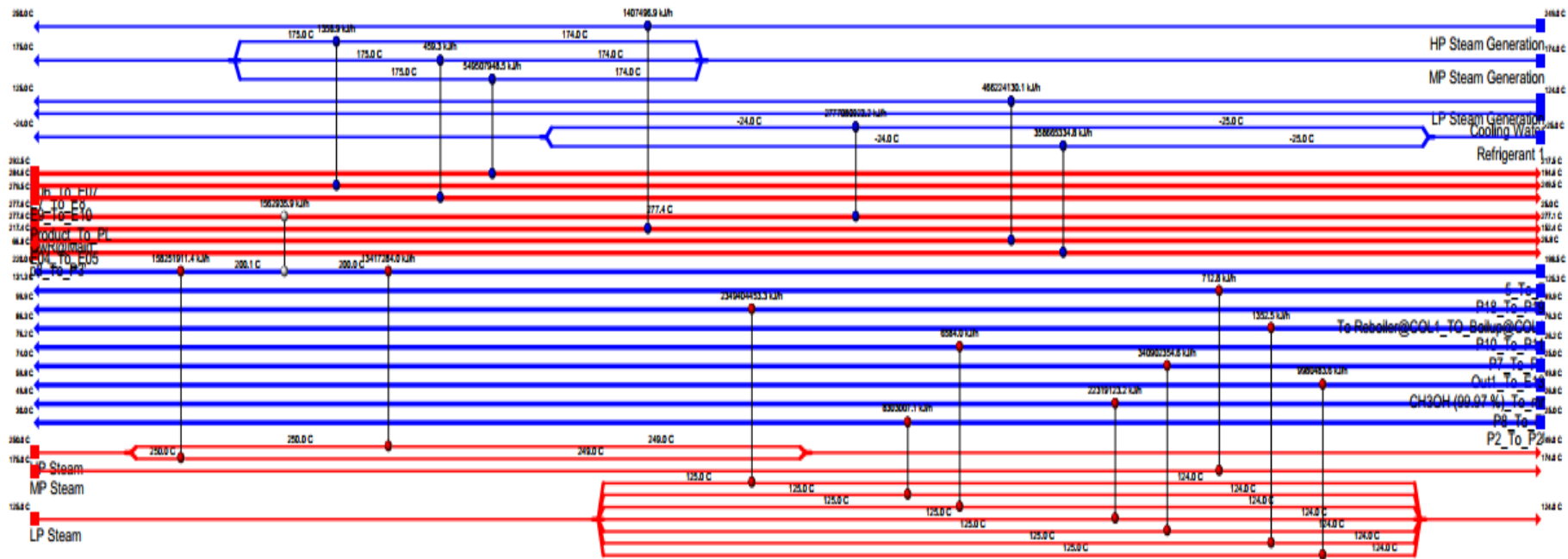


Figure A 3: Profile of HEN-integration of Graaf kinetic model.

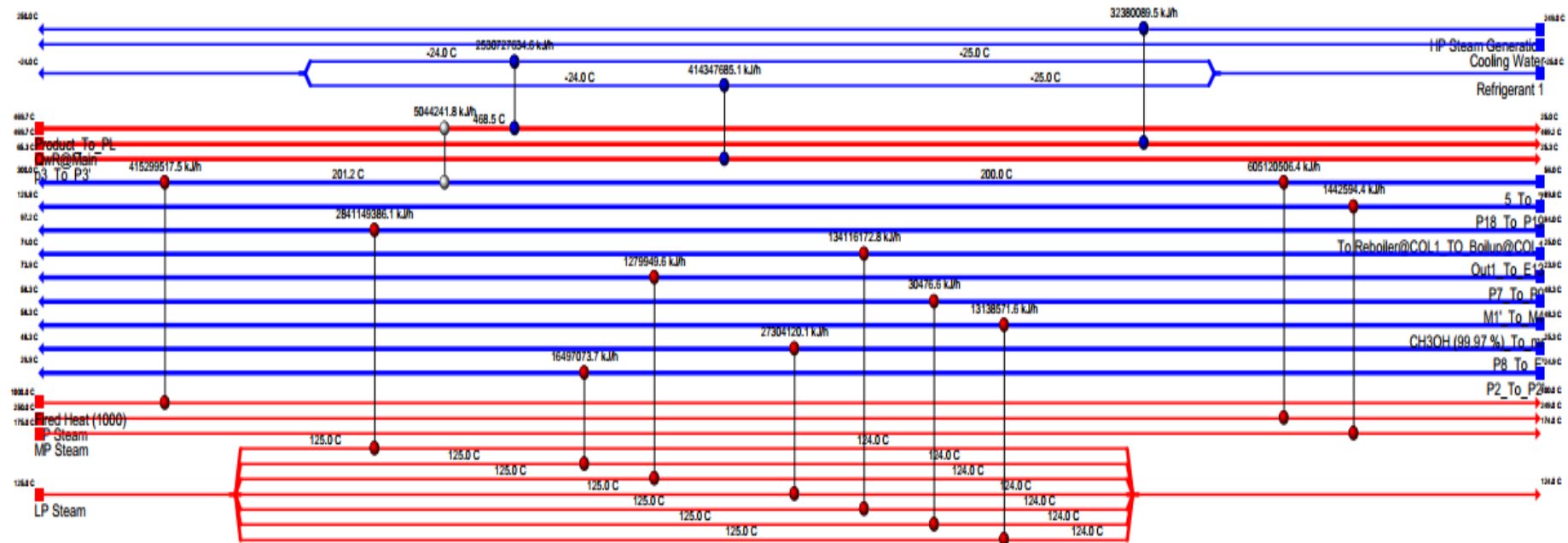


Figure A 4: Profile of HEN-integration of Nestler model.

## APPENDIX 2: TABLE

Table A 1: Total LCMeOH of methanol plant design of all kinetic models.

Model	LCMeOH ( M\$/yr)					
	CAPX	OPEX	OPEX Fixed	Catalyst	Steam	Carbon Dioxide
VBF	182.39	836.19	5.47	0.20	208.16	109.79
Ref-Graaf	134.71	465.31	4.041	0.12	159.29	67.96
Graaf	105.59	473.94	3.17	0.09	255.05	52.20
Nstler	41.47	403.27	2.59	0.04	233.54	23.95

LCMeOH (M\$/yr)		
Hydrogen	Electricity	Cooling Water
427.97	109.79	31.60
264.92	67.96	19.56
203.46	52.19	15.03
93.37	23.95	6.89

Table A 2: Total percentage of OPEX of plant design methanol of all KMs.

Model	Total OPEX ( %)						
	OPEX Fixed	Catalyst	Steam	Carbon Dioxide	Hydrogen	Electricity	Cooling Water
VBF	0.61	0.02	23.31	12.29	47.9259	12.21	3.54
Ref-Graaf	0.69	0.02	27.28	11.64	45.37	11.64	3.35
Graaf	0.55	0.02	43.88	8.98	35.01	8.98	2.59
Nstler	0.67	0.01	60.76	6.23	24.29	6.23	1.79

<b>Name:</b>	Joaquim Paulo Samuel
<b>Permanent Address:</b>	Maputo, Maxaquene-D, AV FPLM
<b>Email Address:</b>	<a href="mailto:joaquimpsamuel@gmail.com">joaquimpsamuel@gmail.com</a>
<b>Education:</b>	Bachelor of Science in Industrial Chemistry
<b>Affiliation:</b>	Society of Petroleum Engineers